

# Reconstructing Biological Pathways by Applying Selective Incremental Learning to (Very) Small Language Models

Pranta Saha  
Vaccine and Infectious  
Disease Organization  
University of Saskatchewan  
Saskatoon, SK, Canada  
[prs527@mail.usask.ca](mailto:prs527@mail.usask.ca)

Neeraj Dhar  
Vaccine and Infectious  
Disease Organization  
University of Saskatchewan  
Saskatoon, SK, Canada  
[neeraj.dhar@usask.ca](mailto:neeraj.dhar@usask.ca)

Joyce Reimer  
Vaccine and Infectious  
Disease Organization  
University of Saskatchewan  
Saskatoon, SK, Canada  
[joyce.reimer@usask.ca](mailto:joyce.reimer@usask.ca)

Jeffrey Chen  
Vaccine and Infectious  
Disease Organization  
University of Saskatchewan  
Saskatoon, SK, Canada  
[jeffrey.chen@usask.ca](mailto:jeffrey.chen@usask.ca)

Brook Byrns  
Advanced Research  
Computing  
University of Saskatchewan  
Saskatoon, SK, Canada  
[brook.byrns@usask.ca](mailto:brook.byrns@usask.ca)

Steven Rayan  
Centre for Quantum  
Topology and Its  
Applications (quanTA)  
University of Saskatchewan  
Saskatoon, SK, Canada  
[steven.rayan@usask.ca](mailto:steven.rayan@usask.ca)

Connor Burbridge  
Advanced Research  
Computing  
University of Saskatchewan  
Saskatoon, SK, Canada  
[connor.burbridge@usask.ca](mailto:connor.burbridge@usask.ca)

Gordon Broderick  
Vaccine and Infectious  
Disease Organization  
University of Saskatchewan  
Saskatoon, SK, Canada  
[awr794@mail.usask.ca](mailto:awr794@mail.usask.ca)

## ABSTRACT

The use of generative artificial intelligence (AI) models is becoming ubiquitous in many fields. Though progress continues to be made, general purpose large language AI models (LLM) show a tendency to deliver creative answers, often called “hallucinations”, which have slowed their application in the medical and biomedical fields where accuracy is paramount. We propose that the design and use of much smaller, domain and even task-specific LM may be a more rational and appropriate use of this technology in biomedical research. In this work we apply a very small LM by today’s standards to the specialized task of predicting regulatory interactions between molecular components to fill gaps in our current understanding of intracellular pathways. Toward this we attempt to correctly posit known pathway-informed interactions recovered from manually curated pathway databases by selecting and using only the most informative examples as part of an active learning scheme. With this example we show that a small (~110 million parameters) LM based on a Bidirectional Encoder Representations from Transformers (BERT) architecture can propose molecular interactions relevant to tuberculosis persistence and transmission with over 80% accuracy using less than 25% of the ~520 regulatory relationships in question. Using information entropy as a metric for the iterative selection of new tuning examples, we also find that increased accuracy is driven by favoring the use of the incorrectly assigned statements with the highest certainty (lowest entropy). In contrast, the concurrent use

Permission to make digital or hard copies of part or all of this work for personal or classroom use is granted without fee provided that copies are not made or distributed for profit or commercial advantage and that copies bear this notice and the full citation on the first page. Copyrights for third-party components of this work must be honored. For all other uses, contact the owner/author(s).

ACM BCB ’25, October, 2025, Philadelphia, Pennsylvania, USA

© 2025 Copyright held by the owner/author(s).

of correct but least certain examples contributed little and may have even been detrimental to the learning rate.

## KEYWORDS

generative AI, BERT, large language models, small language models, active learning, information entropy, regulatory interactions

## 1 Introduction

The presence and use of generative artificial intelligence (AI), in particular pretrained Large Language Models (LLM), is growing rapidly in an ever-expanding range of fields, becoming even ubiquitous in some [1]. Still, there remain significant challenges to their use including high energy costs, data privacy concerns, and the lack of trustworthiness, rigorous logic and transparency [1]. The latter are of special concern in high-risk fields such as medicine where accuracy supported by established facts is paramount and the consequences of a “flight of fancy” can be severe and even life-threatening [2]. Even in the fields of pharmaceutical and biomedical research, pursuing an unsubstantiated lead can be very costly in both time and resources. Despite advances in explainable AI (XAI) directed at improving transparency, the detection and mitigation of these hallucinations often fail to generalize well across datasets, suggesting again that truthfulness may not be universal but rather contextual and multifaceted [3, 4]. In fairness, very large general-purpose models are expected to cover an incredibly broad range of topics undoubtedly leading to immense hunger for data [5] and an almost unavoidably superficial understanding that lends itself to fanciful best guesses or hallucinations. Attempting to escape the adage “Jack of all trades, master of none”, the development and use of domain-specific LLM has emerged as a potentially promising strategy for improving accuracy and believability.

However, so awash with superficial common knowledge are LLM, that attempts at redirecting the latter to more focused domains have been shown in certain circumstances to further increase their appetite for hallucination [4]. The sheer size of such models imparts a significant inertia to altering their foundational beliefs, or calibrated parameter sets, to refocus and tune to new data that is too specialized or too far outside topics represented in their pre-training data sets [6].

In this work, we pursue a highly focused task in a very narrow domain, that involves the reconstruction of biological molecular pathways. As we do not require our model to generate examples outside the immediate domain of molecular cell biology, we can readily take advantage of the known improvements in accuracy associated with domain-specific models. Moreover, this narrow focus also allows for the use of smaller models pre-trained on more limited and potentially higher quality training sets. In contrast to current models approaching 10 T parameters in size [7], we explore herein how very small LM, with parameter counts of 3 B, 1 B and 100 M, might respond to iterative tuning with limited amounts of high quality manually curated biological pathway data describing accepted relationships governing the regulation of proteins in living cells. In addition to exploring model size, we show the benefit of sequential incremental tuning on small segments of data using active learning [8], a static variant of the reinforcement learning strategy recently used to great advantage by DeepSeek (Hangzhou, China) [9]. In this specific use case, we find that policies for the selection of new tuning examples that focus on incorrect prediction made with high certainty favor a broader sampling of the statement space, more robustly avoiding over-represented data elements and leading to better generalization. This strategy applied to a very small 100M parameter BERT LM was able to produce molecular relationships with over 80% accuracy using less than 25% of the overall reference set.

## 2 Methods

### 2.1 Language Models

We evaluated two pretrained-language model architectures, namely an autoregressive language model architecture Llama (Meta, Menlo Park, CA), of 2 different sizes, and a masked-language model ‘bert-base-uncased’ (Google, Mountain View, CA). The autoregressive (AR) Llama is a language model based on the Bidirectional Encoder Representations from Transformers (BERT) [10] architecture, but with the variation of using a causal decoder only stack. In other words, it predicts the next token in a sequence given previous tokens using the activation function SwiGLU (Swish-Gated Linear Unit) instead of the standard GeLU or ReLU [11]. Available in a multitude of sizes, we used the Llama 3.2 (text only) variant with 1B parameters as a comparator. The architecture and the number of parameters is summarized in Table 1. Llama 3.2 was pretrained using a context length of 128k on up to 9 trillion tokens of text from publicly available sources across 9 languages.

The second architecture consisted of a base uncased implementation of the BERT language model architecture. We

also considered a transformer-based model, with the main difference versus Llama being its use of an encoder stack, where each layer uses *self-attention* to look at the entirety of the sentence at once. By including sentence segments positioned both before and after each word, this model attempts to better capture the complete context of each word. For our study, we utilized the BERT-base uncased model consisting of 12-layer transformer blocks and 12 heads as well as 768 hidden units for 110 M parameters in total (Table 1). The model was pretrained on BookCorpus, a dataset consisting of 11,038 unpublished books [12] and English Wikipedia [13]. Pretraining was conducted using a Masked Language Model (MLM) [14] protocol whereby a subset of words in a sentence were randomly masked or hidden and the LM asked to predict those missing words.

### 2.2 A biological use case: data collection and processing

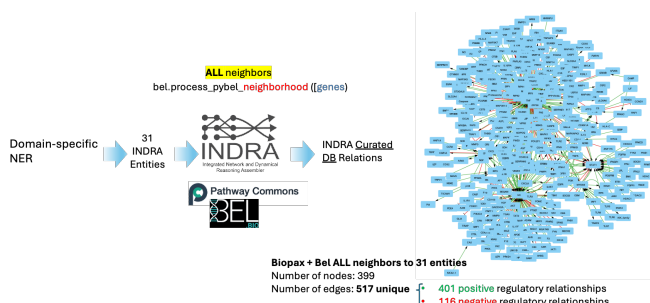
In this preliminary example, we explore the use of LM in proposing as yet undocumented molecular interactions to address gaps in our current understanding of biological pathways important in the response of immune cells to infection by the *Mycobacterium tuberculosis* (Mtb). Specifically, we applied named entity recognition (NER) to two peer-reviewed publications, extracting a list of 22 host proteins involved in persistence of Mtb infection within macrophages [15] and 9 host proteins mediating its transmission by cough [16]. Here, a domain-informed NER was carried out with a custom implementation that used the PyTesseract (Google, Mountain View, CA) [17] for converting PDF files to text and performing Optical Character Recognition (OCR), then recursively applying the LM pretrained in the biomedical domain, such as ‘en\_ner\_jnlpba\_md’, ‘en\_ner\_bc5cdr\_md’, ‘en\_ner\_bionlp13cg\_md’ available under the ScispaCy Python library [18], to extract text elements and label them where appropriate to putative protein names. These text elements were then verified against standard protein names the HGNC (HUGO Gene Nomenclature Committee)[19] and UniProt identifiers [20] and reconciled where possible.

A reference dataset consisting of trusted manually curated relationships linking these 31 proteins to each other and to their first neighbors was constructed by recovering the latter from the Pathway Commons database [21], itself an amalgamation of 23 pathway databases, and the BEL Selventa Large Corpus (<https://github.com/cthoyt/selventa-knowledge>) [22] using the suite of tools available within Integrated Network and Dynamical Reasoning Assembler (INDRA v1.23.0 [23]. Extracted relationships were reconciled into INDRA statements describing a regulatory action of an upstream molecular mediator on a downstream target and labeled as activation, Inhibition, IncreaseAmount, and DecreaseAmount relationship classes. Following the removal of contradictory and redundant INDRA statements, the result was an expanded reference data set consisting now of 399 proteins linked by 517 unique regulatory relationships, with 401 of these classified as positive or

Model Type	Model Name	Year Release	Architecture	Number of Parameters	Context Window	Accessed Through
Autoregressive Language Model	Llama 3.2	2024	Transformer based, Decoder Only Stack	1.3 billion	128000 tokens	ollama/llama3.2:1b
Masked Language Model	bert-base-uncased	2018	Encoder architecture of transformer with 12 layers and 768 hidden layers	110 million	512 tokens	HuggingFace(google-bert/bert-base-uncased)

**Table 1. Language model features.**

upregulation (Uprregulates label) and 116 classified as negative or downregulation (Downregulates label) of a downstream target by an upstream mediator (Figure 1; Supplemental Table S1). These statements taken collectively form a partial regulatory network with the interconnectivity of these proteins described by standard graph theoretical measures in Supplemental Table S2.

**Figure 1. Assembly of a reference data set.** Outline of assembly process used for recovery of entities of interest from text and relationships from manually curated pathway databases.

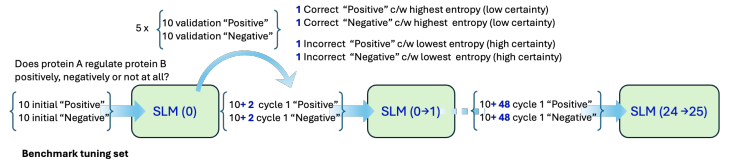
### 2.3 Standardization of data and query formulation

From the post-processed INDRA statements, we created an initial dataset in tabular format with columns: Source, Target and Relationship (upregulates, downregulates). Modern Language Models, such as BERT, are highly robust machine learning models and these models at their core operate on numerical data. They perform mathematical operations such as matrix multiplications, additions, non-linear transformations and cannot directly understand or process text string like “Upregulates” and “Downregulates” as labels. Therefore, to represent categorical information for model training we converted classes to binary labels upregulates to 0 and downregulates to 1. We then use these entries to populate the following LM query (Eq.1).

$$\text{"Does protein [SOURCE\_PROTEIN] regulate protein [TARGET\_PROTEIN] positively or negatively?"} \quad (1)$$

To explore a minimal but informative supervision scenario, we created a baseline data subset consisting of only 10 upregulates and 10 downregulates relations under the constraint that each protein appears only once per class as source and target. The baseline model ( $M(0)$ ) is tuned and a separate random subset

(sampling without replacement) of 10 examples from each class are selected to validate this first model. At each iteration, 2 incorrectly assigned statements are selected from each class based on criteria described below, added to the base tuning set and the model retuned. As such, the tuning set grows as  $2 \times 10 + \text{iterations} \times (4)$  examples (Figure 2).

**Figure 2. Sequential tuning and data selection.** Repeated sequential cycles of active learning with 100% memory using AdamW optimization algorithm using new examples selected as highly confident (low information entropy) but incorrect assignments.

### 2.4 Entropy-based sample selection

To assess the level of certainty with which each validation query is assigned to weak or strong affinity class, we first use the Softmax activation function to transform and normalize the LM raw output scores, also known as “logits”, into a probability distribution (Eq. 2) [24]:

$$p_i = \frac{\exp(z_i)}{\sum_j \exp(z_j)} \quad (2)$$

where  $z_i$  is the logit corresponding to class  $i$  normalized to the interval  $[0,1]$ , and where all output values sum up to 1, thereby providing an estimate of the model’s confidence in assigning a query response to that class. The predicted class was determined by selecting the class with highest probability. We then also used the Shannon entropy over the Softmax output distribution to quantify our model’s uncertainty:

$$H(p) = -\sum_{i=1}^n p_i \log_2(p_i) \quad (3)$$

where  $p_i$  is the probability of assignment to the  $i$ -th class. If the Softmax output for a given prediction is highly concentrated on a single class, the entropy will be low, which means the model is very confident about its prediction. If the output is spread more evenly across multiple classes, the entropy will be high, which will mean the model is uncertain about which class the input belongs to. In this work, each query was submitted to the LM in

replicate a total of 10 times to reduce stochastic variation and compute stable average entropy and confidence values.

## 2.5 LM fine tuning

At each iteration, 5 sets of 10 queries (5 per class) were randomly drawn from the unlabeled pool and evaluated by the model in replicate 10 times each. From these predictions, we selected 1 high-entropy correct but uncertain prediction and 1 low-entropy incorrect but certain prediction from each class, resulting in a maximum of 4 new samples per iteration. As high entropy but correct predictions reflect model uncertainty, this initial criteria was intended to provide positive reinforcement and encourage boundary refinement. Conversely, low entropy but incorrect predictions reflect model overconfidence and their selection for tuning is intended to provide negative reinforcement and the correction of misadjusted beliefs. Selected samples were appended to the training dataset and marked as "used" to avoid re-selection in future iterations. In this cumulative tuning set, both pre-existing and new additions are assigned the same weight supporting a 100% persistent memory framework.

After each selection round, the model was fine-tuned on the updated dataset for 3 epochs using the AdamW optimizer (learning rate:  $2e-5$ ,  $\epsilon = 1e-8$ ) [25]. We used Ray Tune, a widely recognized Python library for distributed hyperparameter optimization [26], to explore search spaces for learning rate, epochs, batch size and weight decay. Models were fine-tuned on both unique and random datasets under identical conditions to assess performance across different data configurations. The hyperparameter selection is summarized in Table 2. Tuning was conducted with a batch size of 8, and validation accuracy was recorded using a consistent held-out validation set. This iterative cycle was repeated for twenty-five iterations.

Hyperparameter	Search Space	Best Value
Optimizer	AdamW	AdamW
Weight Decay	$0.1, 0.01, 0.001$	0.01
Learning Rate	$1e-5 - 5e-5$	$3.00B-05$
Batch Size	4, 8, 16	8
Epochs	2, 4, 8	4
Device	CUDA	CUDA

**Table 2. Hyperparameter selection for BERT model tuning using AdamW search algorithm.**

## 3 Results

### 3.1 Zero-shot inference with small and very small LM

To assess the out-of-the-box performance of both small and very small general-purpose LM on a specialized task with only one round of fine-tuning, we conducted a zero-shot inference task tailored to their respective architectures. Llama (version 3.2 1B) is an autoregressive generative language model, capable of processing open-ended prompts without requiring explicit formatting or fine-tuning. Therefore, we formulated the question

as: "Does protein [SOURCE\_PROTEIN] regulate protein [TARGET\_PROTEIN] positively or negatively?". The model was expected to generate a direct answer (e.g. "positively" or "negatively"), reflecting its understanding of directed regulatory action. Since BERT (bert-base-uncased) is a masked language model (MLM), it requires contextualized input with a token to predict. To guide the model's understanding of protein-protein regulatory interactions, we first provided 10 example sentences, such as: "STAT3 positively regulates ERK", "TLR4 negatively regulates TNF". These question-and-answer examples served as a contextual priming. The model was then queried using the format: "Does protein [SOURCE\_PROTEIN] regulate protein [TARGET\_PROTEIN] positively or negatively? It regulates it [MASK]." Here, the model predicted the masked token, producing an output of either "positively" or "negatively" based on the learned context.

In these limited evaluations, we fine-tuned each LM on 80% of the examples in the smallest class or 93 positive regulation and 93 negative regulation examples. We then submitted the remaining 20% or 23 randomly selected source and target protein pairs as validation queries, replicating this 3 times (Figure 3). The 1B parameter Llama 3.2 LM demonstrated an overwhelming bias to one class, delivering an overall accuracy of 50% (0.43 std. error) with a low entropy of 0.43 for each class underscoring a high certainty of these class assignments (Supplemental Table S3). The much smaller BERT uncased base model delivered an equivalent albeit slightly higher accuracy (54%,  $p=0.27$ ) but with a much more balanced performance and with a significantly higher uncertainty (entropy of 0.95, 0.91 vs 0.43,  $p=0.03, 0.04$ ).

### 3.2 Sequential active learning in BERT base LM

Given the equivalent or better zero-shot performance offered by the much smaller BERT LM, we next then assessed how performance might improve further with additional rounds of tuning using minimal amounts of new data carefully selected. As described in Section 2.5 we randomly selected a baseline initial fine-tuning subset of data consisting of 10 example queries from each class. These were used in a first round of fine-tuning of the out-of-the-box BERT base uncased LM, with performance evaluated against 10 validation queries never before seen by the LM randomly selected from each class. Uncertainty in the form of information entropy was computed for each predicted validation set assignment. In a first experiment we select for each class the correctly predicted validation set example with the highest entropy and the incorrectly predicted validation set example with the lowest entropy. In other words, the most certain incorrect predictions and the least certain incorrect predictions, when available. This was repeated over incremental fine-tuning 25 cycles in two replicate numerical experiments based on the same initial baseline tuning set with the only difference being the random selection of subsequent validation sets. Initial results suggest that the results can be quite variable with repeat experiments achieving an overall accuracy of 69% to 83% (Figure 4; Table 3), using roughly 21% (109 and 110 of 517 relationship statements) of the overall data available.

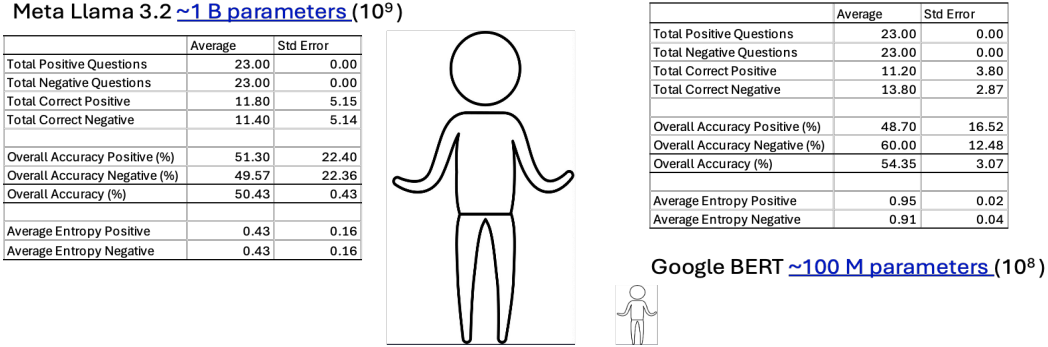


**Figure 3. David and Goliath.** A zero-shot inference using 80% of the overall reference set for tuning and 20% for predictive validation sampled in 5 repeat queries consisting of 23 questions for each class.

To explore the contribution of criteria used in the selection of fine-tuning examples, we examined the trajectory in entropy values of these validation sets across iterations and compared them across experiments. Results shown in Figure 5 show that the trajectory across iterations for entropy values corresponding to incorrect assignments made with high certainty or low entropy in experiment #1 are quite different from those in experiment #2 for both classes. This is especially visible mid-course in iterations 10 through 20 where entropy values for experiment #2 assignments are markedly higher (less certain). In comparison, the trajectories for entropy values assigned to correct assignments made with low

certainty or high entropy essentially overlap in experiments #1 and #2. As the distinguishing feature between experiments #1 and #2 appear driven by fluctuations in the entropy of incorrect and overconfident assignments we attempted to leverage this effect further by focusing on these overconfident assignments only and increasing their number. In a new round of experiments, we now select the 2 incorrect assignments made in each class with the lowest and second lowest entropy values only. Focusing only on the addition of 4 incorrect and overconfident examples at each iteration we now obtain an overall accuracy exceeding 90% using

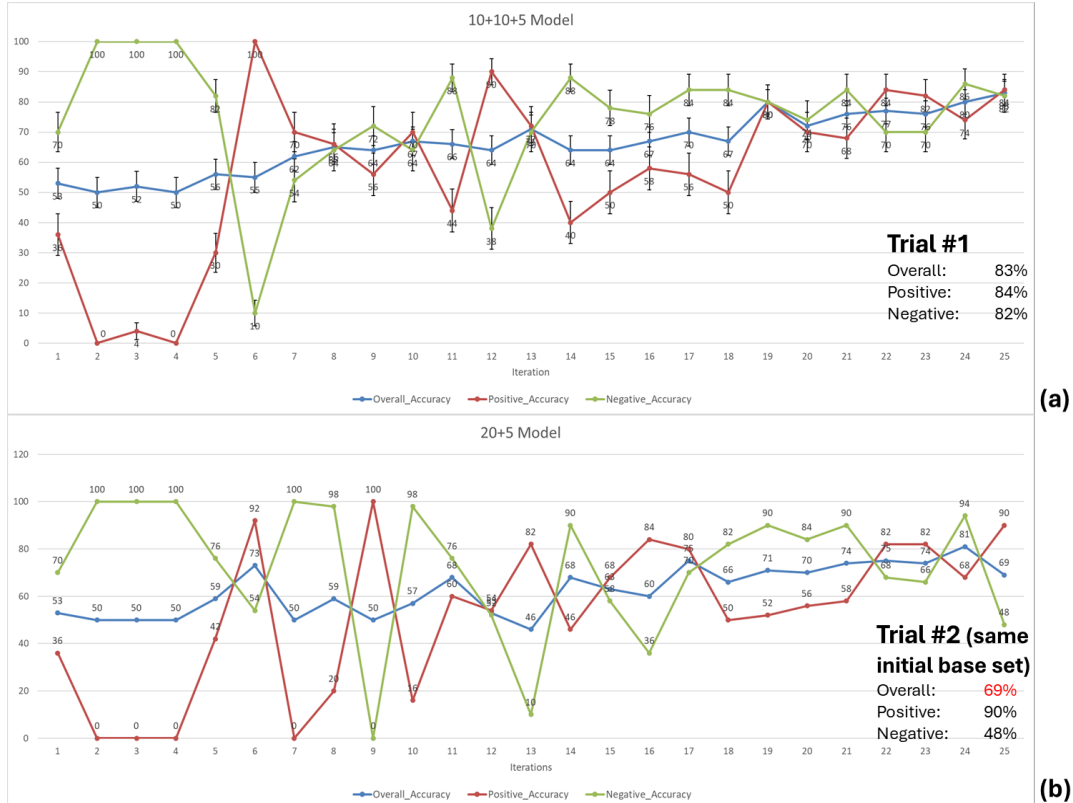


**Figure 4. A joint reward and penalty strategy.** Predictive accuracy achieved with incremental active learning using both underconfident and overconfident examples.

	Correct high E + incorrect low E					Incorrect low E only					
	Trial #1	Trial #2	Trial #3	Average	Std Error	Trial #1	Trial #2	Trial #3	Average	Std Error	p value
Positive Accuracy	84	90	74	82.67	4.67	88	80	100	89.33	5.81	0.424
Negative Accuracy	82	48	76	68.67	10.48	94	100	96	96.67	1.76	0.112
Overall Accuracy	83	69	75	75.67	4.06	91	90	98	93.00	2.52	<b>0.030</b>
Unique Sources											
Edge Count > 1	27	26	32	28.33	1.86	26	32	29	29.00	1.73	0.806
Edge Count =1	16	21	26	21.00	2.89	23	19	15	19.00	2.31	0.619
Unique Targets											
Edge Count > 1	30	26	21	25.67	2.60	28	20	20	22.67	2.67	0.466
Edge Count =1	<u>44</u>	<u>40</u>	40	41.33	1.33	<u>47</u>	37	38	40.67	3.18	0.860
Total Unique	117	113	119	116.33	1.76	124	108	102	111.33	6.57	0.530
Positive Samples Added	47	45	48	46.67	0.88	50	43	37	43.33	3.76	0.471
Negative Samples Added	47	45	47	46.33	0.67	47	39	36	40.67	3.28	0.223
Total samples	94	90	95	93.00	1.53	97	82	73	84.00	7.00	0.326

**Table 3. Summary of active learning results.**

only 23% (117 out of 517 relationship statements) of the overall data available over the same 25 tuning cycles (Figure 6; Table 3).

### 3.3 Selecting informative learning subsets

To better understand how differences in example selection criteria or policy affect learning rate and accuracy, we examined the properties of the examples selected as informative across the 25 fine-tuning iterations. The representation of each molecular species in the role of upstream mediator or downstream target is a product of its location and connectivity as a node in the greater regulatory interaction network. The node level statistics describing the overall connectivity (total edge count), the number of upstream mediators (total indegree), the number of downstream targets (total outdegree), and other connectivity metrics of each node are described in Table S2. Unsurprisingly, inflammatory immune master regulators like TNF and IL6 have the highest connectivity in this network, regulating 177 and 67 downstream targets respectively, which in turn makes them high frequency query subject proteins in the reference set. Likewise, they also rank highly as downstream targets as do STAT1, CRP and MYD88 to a lesser extent, making these well represented as query object proteins in the reference set. The relevance of this over-representation to selection during active learning may be assessed by examining the specific subset of statements extracted over the 25 iterations. Results summarized in Table 3 show that overall predictive accuracy was significantly higher for the policy using only incorrect predictions made with low entropy or high certainty (93.0% vs 75.7%, p=0.03). In examining each regulatory class, we find that while assignment to a positive class was similar in accuracy (82.7% vs 89.3%, p=0.424) across policies, the difference in assignment to a negative class was much more

noticeable (68.7% vs 96.7%, p=0.112), though not statistically significant. In looking more closely at the samples selected by each policy, we found that on average the focus on incorrect low entropy examples resulted in the recruitment of somewhat fewer not more learning examples (84 vs 93, p=0.326) though again the variability was such that this difference did not achieve statistical significance. The composition of these learning sets was quite similar in terms of the overall number of unique molecular species selected (116 and 111 species). Likewise, differences in the frequency with which high versus low connectivity source and target species were selected across policies was unremarkable (Supplemental Table S4) even when examining those species uniquely selected by one policy or the other (Supplemental Table S5). However, when examining the neighborhood connectivity of the species selected differentially in one policy over the other, we find that the use of only incorrect low entropy examples appears to favor a markedly higher sampling of target species connected specifically to network hub mediators (Supplemental Table S5). Indeed, in those few reference set relationships that these species do maintain, they appear as targets of very well-connected master regulators (e.g. TNF with 177 downstream targets). In this example, the policy of selecting only incorrect predictions made with low entropy or high confidence uniquely recruited 24 hub-mediated species compared to 16 such species for the rival policy of also considering low confidence or high entropy but correct predictions.

## 4 Discussion

In this preliminary exploration we attempt to assess the feasibility of using progressively smaller generative AI Language Models (LM) to propose regulatory relationships between

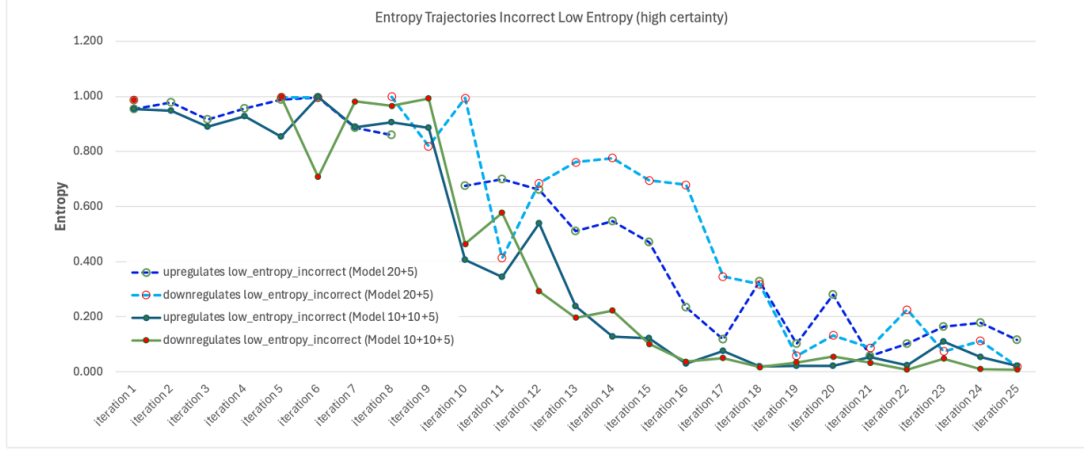


**Figure 5. Contributing policy elements.** Selection of overconfident examples is distinguishing feature in better performing active learning trial.

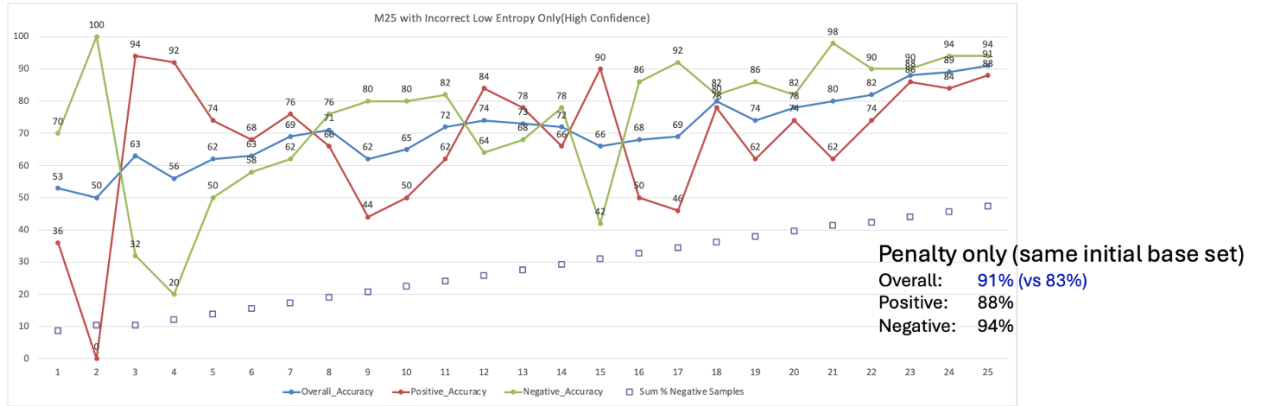


**Figure 6. A reward focused approach.** Predictive accuracy using a penalty-based approach selecting only high confidence but incorrect learning examples.

molecules currently missing from our understanding of biological pathways. Using a set of regulatory relationships extracted from manually curated databases as a reference truth, we show that even when tuned on 80% of the available data, the 100M parameter BERT model performs at least as well in terms of predictive accuracy as the much larger Llama 3.2 1B and 3 B LMs. Interestingly, the latter display a significantly higher level of certainty (lower entropy) despite delivering essentially random class assignments (~50% accuracy). With added size and complexity delivering little value in this use case, we then show that even the parsimonious 100M parameter basic BERT model can achieve classification accuracies in excess of 80% using little more than 20% of the overall data if we incrementally introduce small numbers of well-chosen examples instead of indiscriminate tuning on much larger amounts of data. This in and of itself is not all that surprising and the advantages of incremental elective tuning in delivering high accuracies at low resource usage have drawn significant industry attention recently as demonstrated by DeepSeek's (Hangzhou, China) [9] use of reinforcement learning. In the current analysis, we use active learning (AL) as a

framework for the incremental selection of informative tuning examples which might be described as being akin to a static form of reinforcement learning.

Given the significant and often dramatic reduction in data requirement, there is a rapidly evolving focus on comparing various policies for the selection of the most informative examples with the most fundamental approaches using metrics for prediction uncertainty, as well as example diversity and similarity [27]. Here we focused on prediction uncertainty [28] as a selection metric where the standard selection strategy consists of recruiting examples with the most uncertain prediction or highest entropy. However, as labeled data was available, we compared the selection of high entropy but correctly predicted examples with the recruitment of low entropy but incorrectly classified examples. While labels have been used as a measure of consistency to infer uncertainty [29] and estimates of correctness based on greedy decoding have been used to adjust uncertainty measures [30], there is little work exploring the direct use of true labels in conjunction with an information theoretic measure such as entropy. Indeed, our exploratory analysis suggests that low

certainty, but correct predictions may be less informative than incorrect predictions made with high certainty. Focusing exclusively on the latter appears to favor a more active sampling of species that though poorly connected to other species overall, are selectively mediated by well-connected master regulators. Such well-connected mediators would appear frequently as source terms in the reference query set, which may explain the low entropy values or high certainty of validation statements including these mediators as sources. As a result, predictions might inherit a false confidence (low entropy) from such a frequently occurring source term while struggling to predict a rarely occurring target term or poorly connected target species. This early observation may serve to further modify, inform and streamline the label-aware strategy proposed by Lin et al. [30], offering an alternative to the greedy decoding model that may deliver an even more efficient use of data. Indeed, the concurrent prediction of correctness used by Lin [30] might be modified to focus on infrequent target terms leading to generally incorrect answers by leveraging our knowledge of the small world or hub-centric network architectures common in biology [31]. Such a modified label-aware strategy could be used as a means of proposing the next best query to verify, serving as a means of designing new maximally informative experiments.

Certainly, these observations are derived from a very limited and specific use case and these concepts should be more broadly tested to assess how well they might generalize. In further exploiting the advantages of domain-focused models, a migration from the basic BERT pre-trained model used here to the BioBERT model pre-trained on biomedical content in PubMed would be worth assessing. Regardless of base model, as our group continues to explore definitions and metrics of reliability and trustworthiness, we expect to also enlist concepts from Confident Learning [32]. In addition, while a small reference data set was used here this may not always be the case and efforts will inevitably become focused on improving the compactness of the overall reference set (currently 100% retention) by leveraging parameter-efficient fine-tuning approaches (PEFT) [33] such as LoRa/ QLoRa [34]. Ultimately, these results will help craft more robust approaches for predicting the most compact sets of maximally informative new queries. Specifically, new queries for which no labels exist yet and that, if answered experimentally, would optimally enrich the reference data set.

## ACKNOWLEDGEMENTS

This work was supported by the University of Saskatchewan's Centre for Quantum Topology and Its Applications (quanTA) and by the Vaccine and Infectious Disease Organization (VIDO). VIDO receives operational funding from the Canada Foundation for Innovation (CFI) through the Major Science Initiatives Fund and from the Government of Saskatchewan through Innovation Saskatchewan and the Ministry of Agriculture. The quanTA Centre's high-performance computational work has been advanced through a CFI John R. Evans Leaders Fund grant. We thank the University of Saskatchewan Advanced Research Computing (ARC) team for their efforts and close collaboration in creating an

excellent local environment for this computational work. This article is submitted with the permission of the Director of VIDO.

## REFERENCES

- [1] Zina Chkirkene, Ridha Hamila, Ali Gouisse, and Unal Devrim. 2024. Large Language Models (LLM) in Industry: A Survey of Applications, Challenges, and Trends. In 2024 IEEE 21st International Conference on Smart Communities: Improving Quality of Life using AI, Robotics and IoT (HONET). IEEE, 229-234. DOI: <https://doi.org/10.1109/HONET63146.2024.10822885>
- [2] Pouria Rouzrokh, Bardia Khosravi, Shahriar Faghani, Mana Moassefi, M. Moein Sharifiati, Parsa Rouzrokh, and Bradley Erickson. 2025. A Current Review of Generative AI in Medicine: Core Concepts, Applications, and Current Limitations. *Curr Rev Musculoskelet Med* 18, 7 (Jul 2025), 1-21. DOI: <https://doi.org/10.1007/s12178-025-09961-y>
- [3] Gabrijela Perković, Antun Drobnjak, and Ivica Botički. 2024. Hallucinations in llms: Understanding and addressing challenges. In 2024 47th MIPRO ICT and Electronics Convention (MIPRO). IEEE, 2084-2088. DOI: <https://doi.org/10.1109/MIPRO60963.2024.10569238>
- [4] Hadas Orgad, Michael Toker, Zorik Gekhman, Roi Reichart, Idan Szektor, Hadas Kotek, and Yonatan Belinkov. 2024. Llms know more than they show: On the intrinsic representation of llm hallucinations. arXiv preprint arXiv:2410.02707 (Oct 2024). DOI: <https://doi.org/10.48550/arXiv.2410.02707>
- [5] Pablo Villalobos, Anson Ho, Jaime Sevilla, Tamay Besiroglu, Lennart Heim, and Marius Hobbahn. 2022. Will we run out of data? Limits of LLM scaling based on human-generated data. arXiv preprint arXiv:2211.04325 (Oct 2022). DOI: <https://doi.org/10.48550/arXiv.2211.04325>
- [6] Zorik Gekhman, Gal Yona, Roei Aharoni, Matan Eyal, Amir Feder, Roi Reichart, Jonathan Herzig. (2024). Does fine-tuning LLMs on new knowledge encourage hallucinations?. arXiv preprint arXiv:2405.05904 (May 2024). DOI: <https://doi.org/10.48550/arXiv.2405.05904>
- [7] Mikhail Isaev, Nic McDonald, and Richard Vaduc. 2023. Scaling infrastructure to support multi-trillion parameter LLM training. In Architecture and System Support for Transformer Models (ASSYST@ ISCA 2023).
- [8] Sabit Hassan, Anthony Sicilia, and Malihe Alikhani. 2024. Active Learning for Robust and Representative LLM Generation in Safety-Critical Scenarios. arXiv preprint arXiv:2410.11114 (Oct. 2024). DOI: <https://doi.org/10.48550/arXiv.2410.11114>
- [9] DeepSeek-AI, Daya Guo, Dejian Yang, Haowei Zhang, Junxiao Song, Ruoyu Zhang, et al. 2025. Deepseek-rl: Incentivizing reasoning capability in llms via reinforcement learning. arXiv preprint arXiv:2501.12948 (Jan 2025). DOI: <https://doi.org/10.48550/arXiv.2501.12948>
- [10] Jacob Devlin, Ming-Wei Chang, Kenton Lee, Kristina Toutanova. 2019. Bert: Pre-training of deep bidirectional transformers for language understanding. In Proceedings of the 2019 conference of the North American chapter of the association for computational linguistics: human language technologies, volume 1 (long and short papers). Association for Computational Linguistics, 4171-4186.
- [11] Shiv R. Dubey, Satish K. Singh, and Bidyut B. Chaudhuri. 2022. Activation functions in deep learning: A comprehensive survey and benchmark. *Neurocomputing* 503, 7 (Sep 2022), 92-108. DOI: <https://doi.org/10.1016/j.neucom.2022.06.111>
- [12] Yukun Zhu, Ryan Kiros, Rich Zemel, Ruslan Salakhutdinov, Raquel Urtasun, Antonio Torralba, and Sanja Fidler. 2015. Aligning books and movies: Towards story-like visual explanations by watching movies and reading books. In 2015 Proceedings of the IEEE international conference on computer vision (ICCV). IEEE, 19-27. DOI: <https://doi.ieeecomputersociety.org/10.1109/ICCV.2015.11>
- [13] Lauren A. Maggio, John M. Willinsky, Ryan M. Steinberg, Daniel Mietchen, Joseph L. Wass, and Ting Dong. 2017. Wikipedia as a gateway to biomedical research: The relative distribution and use of citations in the English Wikipedia. *PLoS one* 12, 12 (Dec 2017), e0190046. DOI: <https://doi.org/10.1371/journal.pone.0190046>
- [14] Julian Salazar, Davis Liang, Toan Q. Nguyen, and Katrin Kirchhoff. 2020. Masked language model scoring. In Proceedings of the 58th Annual Meeting of the Association for Computational Linguistics. Association for Computational Linguistics, 2699-2712. DOI: <https://doi.org/10.18653/v1/2020.acl-main.240>
- [15] Bappaditya Dey, and William R. Bishai. 2014. Crosstalk between Mycobacterium tuberculosis and the host cell. *Semin Immunol* 26, 6 (Dec 2014), 486-496. DOI: <https://doi.org/10.1016/j.smim.2014.09.002>
- [16] Kubra F. Naqvi, Stuart B. Mazzzone, and Michael U. Shiloh. 2023. Infectious and inflammatory pathways to cough. *Annu Rev Physiol* 10, 85 (Feb 2023), 71-91. DOI: <https://doi.org/10.1146/annurev-physiol-031422-092315>
- [17] Prakhar Sisodia and Syed W.A. Rizvi. 2023. Optical character recognition development using python. *J Inform Electr Electron Eng* 4, 3 (Nov 2023), 1-3. DOI: <http://dx.doi.org/10.5406/jieee.2023.75>
- [18] Mark Neumann, Daniel King, Iz Beltagy, and Waleed Ammar. 2019. Scispacy: fast and robust models for biomedical natural language processing. In Proceedings of the 18th BioNLP Workshop and Shared Task. Association for

- Computational Linguistics, 319-327. DOI: <https://doi.org/10.18653/v1/W19-5034>
- [19] Tina A. Eyre, Fabrice Ducluzeau, Tam P. Sneddon, Sue Povey, Elspeth A. Bruford, and Michael J. Lush. 2006. The HUGO gene nomenclature database, 2006 updates. *Nucleic Acids Res*, 34, suppl\_1 (Jan 2006), D319-21. DOI: <https://doi.org/10.1093/nar/gkj147>
- [20] The UniProt Consortium. 2015. UniProt: a hub for protein information. *Nucleic Acids Res*, 43, D1 (Jan 2015), D204-12. DOI: <https://doi.org/10.1093/nar/gku989>
- [21] Igor Rodchenkov, Ozgun Babur, Augustin Luna, Bulent A. Aksoy, Jeffrey V. Wong, Dylan Fong, et al. 2020. Pathway Commons 2019 Update: integration, analysis and exploration of pathway data. *Nucleic Acids Res*, 48, D1 (Jan 2020), D489-97. DOI: <https://doi.org/10.1093/nar/gkz946>
- [22] Charles T. Hoyt, Daniel Domingo-Fernández, Rana Aldisi, Lingling Xu, Kristian Kolpeja, Sandra Spalek, et al. 2019. Re-curation and rational enrichment of knowledge graphs in Biological Expression Language. *Database*, 2019, (June 2019), baz068. DOI: <https://doi.org/10.1093/database/baz068>
- [23] John A. Bachman, Benjamin M. Gyori, and Peter K. Sorger. 2023. Automated assembly of molecular mechanisms at scale from text mining and curated databases. *Mol Syst Biol*, 19, 5 (May 2023), e11325. DOI: <https://doi.org/10.1525/msb.202211325>
- [24] Javier Ferrando, Gabriele Sarti, Arianna Bisazza, and Marta R. Costa-Jussà. 2024. A primer on the inner workings of transformer-based language models. arXiv preprint arXiv:2405.00208 (Apr 2024). DOI: <https://doi.org/10.48550/arXiv.2405.00208>
- [25] Ilya Loshchilov and Frank Hutter. 2017. Decoupled weight decay regularization. arXiv preprint arXiv:1711.05101 (Nov 2017). DOI: <https://doi.org/10.48550/arXiv.1711.05101>
- [26] Richard Liaw, Eric Liang, Robert Nishihara, Philipp Moritz, Joseph E. Gonzalez, and Ion Stoica. 2018. Tune: A research platform for distributed model selection and training. arXiv preprint arXiv:1807.05118 (Jul 2018). DOI: <https://doi.org/10.48550/arXiv.1807.05118>
- [27] Katerina Margatina, Timo Schick, Nikolaos Aletras, and Jane Dwivedi-Yu. 2023. Active learning principles for in-context learning with large language models. arXiv preprint arXiv:2305.14264 (May 2023). DOI: <https://doi.org/10.48550/arXiv.2305.14264>
- [28] Hsiu-Yuan Huang, Yutong Yang, Zhaoxi Zhang, Sanwoo Lee, and Yunfang Wu. 2024. A survey of uncertainty estimation in llms: Theory meets practice. arXiv preprint arXiv:2410.15326 (Oct 2024). DOI: <https://doi.org/10.48550/arXiv.2410.15326>
- [29] Hsiu-Yuan Huang, Zichen Wu, Yutong Yang, Junzhao Zhang, and Yunfang Wu. 2024. Unlocking the power of llm uncertainty for active in-context example selection. arXiv preprint arXiv:2408.09172 (Aug 2024). DOI: <https://doi.org/10.48550/arXiv.2408.09172>
- [30] Qinhong Lin, Linna Zhou, Zhongliang Yang, and Yuang Cai. Label-confidence-aware uncertainty estimation in natural language generation. 2024. arXiv preprint arXiv:2412.07255 (Dec 2024). DOI: <https://doi.org/10.48550/arXiv.2412.07255>
- [31] Stefan Wuchty, Erszébet Ravasz, and Albert-László Barabási. 2006. The architecture of biological networks. In *Complex Systems Science in Biomedicine*. Thomas S. Deisboeck and J. Yasha Kresh (Eds.), Springer New York, NY, 165-81.
- [32] Curtis Northcutt, Lu Jiang, Isaac Chuang. 2021. Confident learning: Estimating uncertainty in dataset labels. *JAIR* 70 (Apr 2021), 1373-411. DOI: <https://doi.org/10.1613/jair.1.12125>
- [33] Lingling Xu, Haoran Xie, Si-Zhao J. Qin, Xiaohui Tao, and Fu L.Wang. 2023. Parameter-efficient fine-tuning methods for pretrained language models: A critical review and assessment. arXiv preprint arXiv:2312.12148 (Dec 2023). DOI: <https://doi.org/10.48550/arXiv.2312.12148>
- [34] Rajvardhan Patil, Priyanka Khot, and Venkat Gudivada. 2025. Analyzing LLAMA3 performance on classification task using LoRA and QLoRA techniques. *Appl Sci* 15, 6 (Mar 2025), 3087. DOI: <https://doi.org/10.3390/app15063087>

**Table S1.** Reference truth statements extracted from Pathway Commons and BEL Large Corpus

Source	Target	Relationship Action
IL6	A2M	Activation
IL6	ABCB1	Activation
TNF	ABCB1	Activation
IL6	ABCC1	Activation
IL6	ABCG2	Activation
IL6	ADAMTS5	Activation
TNF	AGT	Activation
AGT	AIM2	Activation
IL6	AKT1	Activation
TNF	AKT2	Activation
TNF	ALPL	Activation
IL6	ANXA1	Activation
TNF	AREG	Activation
TNF	ATF2	Activation
TNF	ATF3	Activation
TNF	BMP2	Activation
TNF	C1R	Activation
TNF	C3	Activation
TNF	C5AR1	Activation
IL6	C8A	Activation
IL6	C8G	Activation
AP1	CA2	Activation
NKX2-1	CA2	Activation
PKC	CA2	Activation
TNF	CASP1	Activation
TNF	CASP2	Activation
TNF	CASP6	Activation
TNF	CASP7	Activation
MYD88	CASP8	Activation
TNF	CASP8	Activation
IL6	CBL	Activation
TNF	CCL11	Activation
CRP	CCL2	Activation
TNF	CCL2	Activation
TNF	CCL3	Activation
CRP	CCR2	Activation
CEBP	CD14	Activation
IFNA1	CD14	Activation
KITLG	CD14	Activation
PI3K	CD14	Activation
PRKAC	CD14	Activation
TNF	CD14	Activation

IL6	CD163	Activation
IL6	CD1A	Activation
TNF	CD1A	Activation
TNF	CD38	Activation
TNF	CD40	Activation
TNF	CD40LG	Activation
TNF	CD55	Activation
TNF	CD59	Activation
TNF	CD80	Activation
TNF	CD86	Activation
STAT1	CDKN1A	Activation
TNF	CDKN1A	Activation
IL6	CDKN1B	Activation
IL6	CEBPB	Activation
TNF	CEPB	Activation
TNF	CFB	Activation
TNF	CFL2	Activation
TNF	CHUK	Activation
TNF	CK2	Activation
TNF	CLEC3B	Activation
TNF	CLIC4	Activation
IL6	CMA1	Activation
CD32	CRP	Activation
CXCL8	CRP	Activation
ERK	CRP	Activation
HNF1A	CRP	Activation
IL1B	CRP	Activation
IL6	CRP	Activation
LEP	CRP	Activation
NFkappaB	CRP	Activation
p38	CRP	Activation
PTGS2	CRP	Activation
TNF	CRP	Activation
TNF	CSF1	Activation
TNF	CSF2	Activation
TNF	CSF3	Activation
TNF	CTSB	Activation
IL6	CTSL	Activation
IL6	CTSS	Activation
TNF	CX3CL1	Activation
TNF	CXCL10	Activation
TNF	CXCL12	Activation
TNF	CXCL5	Activation
TLR9	CXCL8	Activation
TNF	CXCL9	Activation

TNF	CXCR3	Activation
TNF	DAPK1	Activation
IL6	EGFR	Activation
TNF	EHF	Activation
IRF3	EP300	Activation
PTPA	ERK	Activation
IL6	ESR1	Activation
TNF	F2RL1	Activation
TNF	F2RL3	Activation
<b>TNF</b>	<b>FAS</b>	<b>Activation</b>
TNF	FCER2	Activation
CRP	FCGR1A	Activation
TNF	FCGR3B	Activation
IL6	FN1	Activation
TNF	FOXO4	Activation
TNF	FUT4	Activation
IL6	FYN	Activation
IL6	GBF1	Activation
CAMP	GSK3B	Activation
IL6	HBEGF	Activation
IL6	HCK	Activation
TNF	HIF1A	Activation
TNF	HLA-A	Activation
TNF	HLA-B	Activation
TNF	HLA-C	Activation
TNF	HLA-F	Activation
IL6	HP	Activation
TNF	HSD11B1	Activation
IL6	HSF1	Activation
TNF	HSF1	Activation
IL6	HSP90B1	Activation
HOXD3	IFI16	Activation
IFNG	IFI16	Activation
LIF	IFI16	Activation
RAF1	IFI16	Activation
STAT3	IFI16	Activation
IRF3	IFNA1	Activation
IRF3	IFNB1	Activation
STAT1	IFNG	Activation
TNF	IFNG	Activation
<b>TNF</b>	<b>IKBKB</b>	<b>Activation</b>
TNF	IKBKG	Activation
MYD88	IKK_family	Activation
TNF	IL11	Activation
TNF	IL12A	Activation

TNF	IL12B	Activation
IL6	IL17A	Activation
TNF	IL18	Activation
TNF	IL4R	Activation
ADRB2	IL6	Activation
AGT	IL6	Activation
AHR	IL6	Activation
AP1	IL6	Activation
AR	IL6	Activation
BSG	IL6	Activation
CCL2	IL6	Activation
CD40	IL6	Activation
CD40LG	IL6	Activation
CXCL12	IL6	Activation
EGFR	IL6	Activation
ERBB2	IL6	Activation
F10	IL6	Activation
F2	IL6	Activation
GAB1	IL6	Activation
HCK	IL6	Activation
IFNG	IL6	Activation
IL13	IL6	Activation
IL17A	IL6	Activation
IL17F	IL6	Activation
IL18	IL6	Activation
IL1B	IL6	Activation
IL1R1	IL6	Activation
IL4	IL6	Activation
IL6	IL6	Activation
IL6R	IL6	Activation
IL6ST	IL6	Activation
INS	IL6	Activation
ITGA5	IL6	Activation
KLF7	IL6	Activation
LEPR	IL6	Activation
LMX1B	IL6	Activation
MAPK1	IL6	Activation
NFkappaB	IL6	Activation
NGF	IL6	Activation
OSM	IL6	Activation
p38	IL6	Activation
PARP1	IL6	Activation
PIK3C3	IL6	Activation
PKC	IL6	Activation
PNPT1	IL6	Activation

PTGER4	IL6	Activation
PTK2	IL6	Activation
PTPN11	IL6	Activation
TGFB1	IL6	Activation
TIRAP	IL6	Activation
TLR4	IL6	Activation
TNFRSF1A	IL6	Activation
VEGF	IL6	Activation
XDH	IL6	Activation
IL6	IL6ST	Activation
MYD88	IRAK1	Activation
MYD88	IRAK4	Activation
BEGAIN	IRF3	Activation
CXCL12	IRF3	Activation
IKBKE	IRF3	Activation
MAVS	IRF3	Activation
TICAM1	IRF3	Activation
TLR3	IRF3	Activation
TLR4	IRF3	Activation
MYD88	IRF5	Activation
TLR9	IRF7	Activation
TNF	ITGA6	Activation
TNF	ITGAV	Activation
TNF	JAK	Activation
TNF	JUN	Activation
IL6	KRAS	Activation
IL6	LYN	Activation
TNF	LYZ	Activation
TNF	MAP2K1	Activation
TNF	MAP2K2	Activation
TNF	MAP2K6	Activation
TNF	MAP3K1	Activation
TNF	MAP3K14	Activation
TNF	MAP3K5	Activation
TNF	MAP4K3	Activation
TNF	MAP4K4	Activation
TNF	MAPK1	Activation
IL6	MAPK14	Activation
IL6	MAPK3	Activation
IL6	MAPK7	Activation
TNF	MAPK9	Activation
TNF	MAPKAPK3	Activation
IL6	MAZ	Activation
IL6	MEF2	Activation
IL6	MGAT4B	Activation

IL6	MGAT5	Activation
TNF	MIF	Activation
TNF	MMP1	Activation
TNF	MMP14	Activation
TNF	MMP3	Activation
IL6	MMP9	Activation
TNF	MUC5AC	Activation
IFNG	MYD88	Activation
IRF5	MYD88	Activation
IRF7	MYD88	Activation
TLR1	MYD88	Activation
TLR2	MYD88	Activation
TLR5	MYD88	Activation
TLR6	MYD88	Activation
TLR7	MYD88	Activation
TLR8	MYD88	Activation
TLR9	MYD88	Activation
TNF	MYLK	Activation
TNF	NCAM1	Activation
CD14	NFkappaB	Activation
IL6	NFkappaB	Activation
MYD88	NFkappaB	Activation
TBK1	NFkappaB	Activation
TLR9	NFkappaB	Activation
TNF	NFKB1	Activation
TNF	NFKB2	Activation
TNF	NOS1	Activation
IL6	ORM1	Activation
TNF	PAWR	Activation
TNF	PFN1	Activation
IL6	PHB1	Activation
p38	PI3	Activation
IL6	PI3K	Activation
TNF	PLA2G2A	Activation
TNF	PLAU	Activation
IL6	POMC	Activation
IL6	POU2F1	Activation
TNF	PPP1R15A	Activation
CAMP	PRKAC	Activation
TNF	PRKCI	Activation
TNF	PRKCZ	Activation
IL6	PRKD1	Activation
TNF	Proteasome	Activation
TNF	PSMB9	Activation
TNF	PSME1	Activation

TNF	PTEN	Activation
TNF	PTGES	Activation
TNF	PTGS2	Activation
TNF	PTHLH	Activation
TNF	PTX3	Activation
TNF	RELA	Activation
TNF	RIPK1	Activation
TNF	RIPK2	Activation
TNF	RIPK3	Activation
IL6	RORA	Activation
TNF	SELE	Activation
IL6	SERPINA3	Activation
TNF	SERPINE1	Activation
TNF	SERPING1	Activation
TNF	SERPINH1	Activation
TNF	SLC6A4	Activation
TNF	SLC6A6	Activation
TNF	SMPD1	Activation
STAT1	SOCS1	Activation
TNF	SP1	Activation
TNF	SPP1	Activation
TNF	ST3GAL6	Activation
BMX	STAT1	Activation
EGFR	STAT1	Activation
ETS1	STAT1	Activation
FGFR1	STAT1	Activation
FGFR3	STAT1	Activation
HDAC	STAT1	Activation
HDAC1	STAT1	Activation
HDAC2	STAT1	Activation
HDAC3	STAT1	Activation
IFNA1	STAT1	Activation
IFNG	STAT1	Activation
IFNGR1	STAT1	Activation
IFNL1	STAT1	Activation
IFNL2	STAT1	Activation
IL10	STAT1	Activation
IL6ST	STAT1	Activation
IRAK1	STAT1	Activation
IRF5	STAT1	Activation
JAK2	STAT1	Activation
LPL	STAT1	Activation
MAPK1	STAT1	Activation
MAPK3	STAT1	Activation
NFkappaB	STAT1	Activation

OSM	STAT1	Activation
PDGFRB	STAT1	Activation
PRKCD	STAT1	Activation
PRKCE	STAT1	Activation
PRMT1	STAT1	Activation
RET	STAT1	Activation
TNF	STAT1	Activation
TYK2	STAT1	Activation
IL6	STAT2	Activation
IL6	STAT3	Activation
TNF	STAT3	Activation
TNF	TAP1	Activation
TNF	TAP2	Activation
TLR3	TBK1	Activation
TNF	TGFA	Activation
TNF	THBS1	Activation
TNF	TIMP1	Activation
TNF	TIMP3	Activation
CD14	TLR2	Activation
TNF	TLR2	Activation
TBK1	TLR3	Activation
TGFA	TLR9	Activation
ADAM17	TNF	Activation
ADRB2	TNF	Activation
AGT	TNF	Activation
AGTR1	TNF	Activation
AKR1B1	TNF	Activation
ALOX5	TNF	Activation
AP1	TNF	Activation
BSG	TNF	Activation
Caspase	TNF	Activation
CD14	TNF	Activation
CD40LG	TNF	Activation
CENPJ	TNF	Activation
CHUK	TNF	Activation
CRP	TNF	Activation
DCN	TNF	Activation
DCTN1	TNF	Activation
DHX9	TNF	Activation
EGR4	TNF	Activation
EP300	TNF	Activation
HMGB1	TNF	Activation
HNRNPU	TNF	Activation
HSPA4	TNF	Activation
HSPB1	TNF	Activation

ICMT	TNF	Activation
IFI16	TNF	Activation
IKBKB	TNF	Activation
IKBKG	TNF	Activation
IL17A	TNF	Activation
IL18	TNF	Activation
IL1B	TNF	Activation
IRF9	TNF	Activation
MAP3K1	TNF	Activation
MAP3K7	TNF	Activation
MAPK14	TNF	Activation
MAPK3	TNF	Activation
MMP12	TNF	Activation
NAMPT	TNF	Activation
NFAT	TNF	Activation
NFKappaB	TNF	Activation
NFKBIA	TNF	Activation
NGF	TNF	Activation
NOS3	TNF	Activation
NOX4	TNF	Activation
NRAS	TNF	Activation
OLR1	TNF	Activation
PARP1	TNF	Activation
PDE3B	TNF	Activation
PLA2G4A	TNF	Activation
PTK2	TNF	Activation
RALBP1	TNF	Activation
RIPK2	TNF	Activation
TARDBP	TNF	Activation
TIMP3	TNF	Activation
TLR1	TNF	Activation
TLR2	TNF	Activation
TLR4	TNF	Activation
TONSL	TNF	Activation
TRAF2	TNF	Activation
VEGF	TNF	Activation
TNF	TNFRSF1A	Activation
TNF	TNFRSF1B	Activation
TNF	TP53	Activation
TNF	TRAF1	Activation
TNF	TRAF2	Activation
TNF	TRAF3	Activation
MYD88	TRAF6	Activation
NGF	TRPV1	Activation
TNF	TYMP	Activation

CRP	VCAM1	Activation
TNF	VCAM1	Activation
IL6	VEGFA	Activation
TNF	VEGFA	Activation
TNF	VIM	Activation
TNF	XDH	Activation
TNF	ABCC2	Inhibition
IL6	ADIPOQ	Inhibition
TNF	ADIPOQ	Inhibition
IL6	AHSG	Inhibition
IL6	AKT	Inhibition
PTPA	AKT	Inhibition
IL6	ALB	Inhibition
IL6	APOE	Inhibition
TNF	C3AR1	Inhibition
IL6	CASP9	Inhibition
IFI16	CCND1	Inhibition
TGFB1	CD14	Inhibition
ZNF175	CD14	Inhibition
IL6	CD33	Inhibition
TNF	CP	Inhibition
IL4	CRP	Inhibition
PPARA	CRP	Inhibition
TNF	CST3	Inhibition
TNF	CTNNB1	Inhibition
TNF	EGFR	Inhibition
TNF	ERBB2	Inhibition
TNF	ERG	Inhibition
STAT1	ESR1	Inhibition
TNF	ESR1	Inhibition
IL6	F12	Inhibition
IL6	FOXO1	Inhibition
TNF	FSCN1	Inhibition
IL6	GADD45A	Inhibition
PTPA	GLI3	Inhibition
STAT1	IFNA1	Inhibition
TNF	IGFBP3	Inhibition
IL6	IL1B	Inhibition
BMP6	IL6	Inhibition
ERK	IL6	Inhibition
GH1	IL6	Inhibition
MEOX2	IL6	Inhibition
POMC	IL6	Inhibition
PPARA	IL6	Inhibition
PPARG	IL6	Inhibition

SOCS3	IL6	Inhibition
SOD1	IL6	Inhibition
IL6	INS	Inhibition
TNF	INSR	Inhibition
TNF	JUP	Inhibition
PTPA	MAPK1	Inhibition
TNF	MAPK3	Inhibition
IL6	NCOA1	Inhibition
STAT1	NFkappaB	Inhibition
CRP	NFKBIA	Inhibition
TNF	NFKBIB	Inhibition
TNF	NOS2	Inhibition
TNF	NOS3	Inhibition
TNF	OCLN	Inhibition
PTPA	PDE4	Inhibition
TNF	POU2F1	Inhibition
TNF	PPM1B	Inhibition
TNF	PROCR	Inhibition
IL6	PROS1	Inhibition
TNF	RB1	Inhibition
TNF	RETN	Inhibition
TNF	SCARB1	Inhibition
TNF	SCD	Inhibition
TNF	SLC10A1	Inhibition
TNF	SLC2A4	Inhibition
TNF	SLCO1A2	Inhibition
ADRB	STAT1	Inhibition
PIAS1	STAT1	Inhibition
PTPN11	STAT1	Inhibition
SOCS3	STAT1	Inhibition
CRP	TERT	Inhibition
TNF	TFAP2C	Inhibition
TNF	THBD	Inhibition
ADIPOQ	TNF	Inhibition
ADRB	TNF	Inhibition
AMPK	TNF	Inhibition
EGF	TNF	Inhibition
GSK3B	TNF	Inhibition
IFNB1	TNF	Inhibition
IL10	TNF	Inhibition
IL10RA	TNF	Inhibition
IL13	TNF	Inhibition
INS	TNF	Inhibition
P2RY6	TNF	Inhibition
PEBP1	TNF	Inhibition

PIAS3	TNF	Inhibition
PNPLA3	TNF	Inhibition
POU2F1	TNF	Inhibition
PRKCH	TNF	Inhibition
PTEN	TNF	Inhibition
PTGS2	TNF	Inhibition
RHOB	TNF	Inhibition
RNF216	TNF	Inhibition
RORA	TNF	Inhibition
SALL4	TNF	Inhibition
SERPINA1	TNF	Inhibition
SERPINA3	TNF	Inhibition
SFTPA1	TNF	Inhibition
SH3BGRL3	TNF	Inhibition
SOD2	TNF	Inhibition
STAT1	TNF	Inhibition
STAT3	TNF	Inhibition
TNFAIP3	TNF	Inhibition
TNFRSF1B	TNF	Inhibition
TXN	TNF	Inhibition
USP31	TNF	Inhibition
VIPR2	TNF	Inhibition
XIAP	TNF	Inhibition
ZFAND5	TNF	Inhibition
ZFP36	TNF	Inhibition

Number of Inhibition Statements  
109  
Number of Activation Statements  
408  
Total Number of Statements  
517

:

***\*\* Indicates statement reconciled across duplicates with majority rule***

**Table S2.** Connectivity properties or relationship statement density of individual sources and targets

ADAMTS5	1	0	1	0.00	0.00	0.00	0.00	0.00	116.00
AIM2	1	0	1	0.00	0.00	0.00	0.00	0.00	3.00
AKT1	1	0	1	0.00	0.00	0.00	0.00	0.00	116.00
AKT2	1	0	1	0.00	0.00	0.00	0.00	0.00	251.00
ALPL	1	0	1	0.00	0.00	0.00	0.00	0.00	251.00
ANXA1	1	0	1	0.00	0.00	0.00	0.00	0.00	116.00
AREG	1	0	1	0.00	0.00	0.00	0.00	0.00	251.00
ATF2	1	0	1	0.00	0.00	0.00	0.00	0.00	251.00
ATF3	1	0	1	0.00	0.00	0.00	0.00	0.00	251.00
BMP2	1	0	1	0.00	0.00	0.00	0.00	0.00	251.00
C1R	1	0	1	0.00	0.00	0.00	0.00	0.00	251.00
C3	1	0	1	0.00	0.00	0.00	0.00	0.00	251.00
C5AR1	1	0	1	0.00	0.00	0.00	0.00	0.00	251.00
C8A	1	0	1	0.00	0.00	0.00	0.00	0.00	116.00
C8G	1	0	1	0.00	0.00	0.00	0.00	0.00	116.00
NKX2-1	0	1	1	0.00	1.00	0.00	1.00	1.00	3.00
CASP1	1	0	1	0.00	0.00	0.00	0.00	0.00	251.00
CASP2	1	0	1	0.00	0.00	0.00	0.00	0.00	251.00
CASP6	1	0	1	0.00	0.00	0.00	0.00	0.00	251.00
CASP7	1	0	1	0.00	0.00	0.00	0.00	0.00	251.00
CBL	1	0	1	0.00	0.00	0.00	0.00	0.00	116.00
CCL11	1	0	1	0.00	0.00	0.00	0.00	0.00	251.00
CCL3	1	0	1	0.00	0.00	0.00	0.00	0.00	251.00
CCR2	1	0	1	0.00	0.00	0.00	0.00	0.00	19.00
CEBP	0	1	1	0.00	0.30	0.00	5.00	3.29	10.00
KITLG	0	1	1	0.00	0.30	0.00	5.00	3.29	10.00
CD163	1	0	1	0.00	0.00	0.00	0.00	0.00	116.00
CD38	1	0	1	0.00	0.00	0.00	0.00	0.00	251.00
CD55	1	0	1	0.00	0.00	0.00	0.00	0.00	251.00
CD59	1	0	1	0.00	0.00	0.00	0.00	0.00	251.00
CD80	1	0	1	0.00	0.00	0.00	0.00	0.00	251.00
CD86	1	0	1	0.00	0.00	0.00	0.00	0.00	251.00
CDKN1B	1	0	1	0.00	0.00	0.00	0.00	0.00	116.00
CFB	1	0	1	0.00	0.00	0.00	0.00	0.00	251.00
CFL2	1	0	1	0.00	0.00	0.00	0.00	0.00	251.00
CK2	1	0	1	0.00	0.00	0.00	0.00	0.00	251.00
CLEC3B	1	0	1	0.00	0.00	0.00	0.00	0.00	251.00
CLIC4	1	0	1	0.00	0.00	0.00	0.00	0.00	251.00
CMA1	1	0	1	0.00	0.00	0.00	0.00	0.00	116.00
CD32	0	1	1	0.00	0.30	0.00	5.00	3.28	19.00
HNF1A	0	1	1	0.00	0.30	0.00	5.00	3.28	19.00
LEP	0	1	1	0.00	0.30	0.00	5.00	3.28	19.00
CSF1	1	0	1	0.00	0.00	0.00	0.00	0.00	251.00
CSF2	1	0	1	0.00	0.00	0.00	0.00	0.00	251.00
CSF3	1	0	1	0.00	0.00	0.00	0.00	0.00	251.00
CTSB	1	0	1	0.00	0.00	0.00	0.00	0.00	251.00
CTSL	1	0	1	0.00	0.00	0.00	0.00	0.00	116.00
CTSS	1	0	1	0.00	0.00	0.00	0.00	0.00	116.00
CX3CL1	1	0	1	0.00	0.00	0.00	0.00	0.00	251.00
CXCL10	1	0	1	0.00	0.00	0.00	0.00	0.00	251.00
CXCL5	1	0	1	0.00	0.00	0.00	0.00	0.00	251.00
CXCL9	1	0	1	0.00	0.00	0.00	0.00	0.00	251.00
CXCR3	1	0	1	0.00	0.00	0.00	0.00	0.00	251.00
DAPK1	1	0	1	0.00	0.00	0.00	0.00	0.00	251.00
EHF	1	0	1	0.00	0.00	0.00	0.00	0.00	251.00
F2RL1	1	0	1	0.00	0.00	0.00	0.00	0.00	251.00
F2RL3	1	0	1	0.00	0.00	0.00	0.00	0.00	251.00
FAS	1	0	1	0.00	0.00	0.00	0.00	0.00	251.00
FCER2	1	0	1	0.00	0.00	0.00	0.00	0.00	251.00
FCGR1A	1	0	1	0.00	0.00	0.00	0.00	0.00	19.00
FCGR3B	1	0	1	0.00	0.00	0.00	0.00	0.00	251.00
FN1	1	0	1	0.00	0.00	0.00	0.00	0.00	116.00
FOXO4	1	0	1	0.00	0.00	0.00	0.00	0.00	251.00
FUT4	1	0	1	0.00	0.00	0.00	0.00	0.00	251.00
FYN	1	0	1	0.00	0.00	0.00	0.00	0.00	116.00
GBF1	1	0	1	0.00	0.00	0.00	0.00	0.00	116.00
HBEGF	1	0	1	0.00	0.00	0.00	0.00	0.00	116.00
HIF1A	1	0	1	0.00	0.00	0.00	0.00	0.00	251.00
HLA-A	1	0	1	0.00	0.00	0.00	0.00	0.00	251.00
HLA-B	1	0	1	0.00	0.00	0.00	0.00	0.00	251.00
HLA-C	1	0	1	0.00	0.00	0.00	0.00	0.00	251.00
HLA-F	1	0	1	0.00	0.00	0.00	0.00	0.00	251.00
HP	1	0	1	0.00	0.00	0.00	0.00	0.00	116.00
HSD11B1	1	0	1	0.00	0.00	0.00	0.00	0.00	251.00
HSP90B1	1	0	1	0.00	0.00	0.00	0.00	0.00	116.00
HOXD3	0	1	1	0.00	0.28	0.00	5.00	3.52	7.00
LIF	0	1	1	0.00	0.28	0.00	5.00	3.52	7.00
RAF1	0	1	1	0.00	0.28	0.00	5.00	3.52	7.00
IKK_family	1	0	1	0.00	0.00	0.00	0.00	0.00	16.00
IL11	1	0	1	0.00	0.00	0.00	0.00	0.00	251.00
IL12A	1	0	1	0.00	0.00	0.00	0.00	0.00	251.00
IL12B	1	0	1	0.00	0.00	0.00	0.00	0.00	251.00
IL4R	1	0	1	0.00	0.00	0.00	0.00	0.00	251.00
AHR	0	1	1	0.00	0.28	0.00	6.00	3.52	116.00
AR	0	1	1	0.00	0.28	0.00	6.00	3.52	116.00
F10	0	1	1	0.00	0.28	0.00	6.00	3.52	116.00
F2	0	1	1	0.00	0.28	0.00	6.00	3.52	116.00
GAB1	0	1	1	0.00	0.28	0.00	6.00	3.52	116.00
IL17F	0	1	1	0.00	0.28	0.00	6.00	3.52	116.00
IL1R1	0	1	1	0.00	0.28	0.00	6.00	3.52	116.00
IL6R	0	1	1	0.00	0.28	0.00	6.00	3.52	116.00
ITGA5	0	1	1	0.00	0.28	0.00	6.00	3.52	116.00
KLF7	0	1	1	0.00	0.28	0.00	6.00	3.52	116.00
LEPR	0	1	1	0.00	0.28	0.00	6.00	3.52	116.00
LMX1B	0	1	1	0.00	0.28	0.00	6.00	3.52	116.00
PIK3C3	0	1	1	0.00	0.28	0.00	6.00	3.52	116.00
PNPT1	0	1	1	0.00	0.28	0.00	6.00	3.52	116.00
PTGER4	0	1	1	0.00	0.28	0.00	6.00	3.52	116.00
TIRAP	0	1	1	0.00	0.28	0.00	6.00	3.52	116.00
IRAK4	1	0	1	0.00	0.00	0.00	0.00	0.00	16.00
BEGAIN	0	1	1	0.00	0.22	0.00	6.00	4.47	10.00

IKBKE	0	1	1	0.00	0.22	0.00	6.00	4.47	10.00
MAVS	0	1	1	0.00	0.22	0.00	6.00	4.47	10.00
TICAM1	0	1	1	0.00	0.22	0.00	6.00	4.47	10.00
ITGA6	1	0	1	0.00	0.00	0.00	0.00	0.00	251.00
ITGAV	1	0	1	0.00	0.00	0.00	0.00	0.00	251.00
JAK	1	0	1	0.00	0.00	0.00	0.00	0.00	251.00
JUN	1	0	1	0.00	0.00	0.00	0.00	0.00	251.00
KRAS	1	0	1	0.00	0.00	0.00	0.00	0.00	116.00
LYN	1	0	1	0.00	0.00	0.00	0.00	0.00	116.00
LYZ	1	0	1	0.00	0.00	0.00	0.00	0.00	251.00
MAP2K1	1	0	1	0.00	0.00	0.00	0.00	0.00	251.00
MAP2K2	1	0	1	0.00	0.00	0.00	0.00	0.00	251.00
MAP2K6	1	0	1	0.00	0.00	0.00	0.00	0.00	251.00
MAP3K14	1	0	1	0.00	0.00	0.00	0.00	0.00	251.00
MAP3K5	1	0	1	0.00	0.00	0.00	0.00	0.00	251.00
MAP4K3	1	0	1	0.00	0.00	0.00	0.00	0.00	251.00
MAP4K4	1	0	1	0.00	0.00	0.00	0.00	0.00	251.00
MAPK7	1	0	1	0.00	0.00	0.00	0.00	0.00	116.00
MAPK9	1	0	1	0.00	0.00	0.00	0.00	0.00	251.00
MAPKAPK3	1	0	1	0.00	0.00	0.00	0.00	0.00	251.00
MAZ	1	0	1	0.00	0.00	0.00	0.00	0.00	116.00
MEF2	1	0	1	0.00	0.00	0.00	0.00	0.00	116.00
MGAT4B	1	0	1	0.00	0.00	0.00	0.00	0.00	116.00
MGAT5	1	0	1	0.00	0.00	0.00	0.00	0.00	116.00
MIF	1	0	1	0.00	0.00	0.00	0.00	0.00	251.00
MMP1	1	0	1	0.00	0.00	0.00	0.00	0.00	251.00
MMP14	1	0	1	0.00	0.00	0.00	0.00	0.00	251.00
MMP3	1	0	1	0.00	0.00	0.00	0.00	0.00	251.00
MMP9	1	0	1	0.00	0.00	0.00	0.00	0.00	116.00
MUC5AC	1	0	1	0.00	0.00	0.00	0.00	0.00	251.00
TLR5	0	1	1	0.00	0.25	0.00	6.00	3.97	16.00
TLR6	0	1	1	0.00	0.25	0.00	6.00	3.97	16.00
TLR7	0	1	1	0.00	0.25	0.00	6.00	3.97	16.00
TLR8	0	1	1	0.00	0.25	0.00	6.00	3.97	16.00
MYLK	1	0	1	0.00	0.00	0.00	0.00	0.00	251.00
NCAM1	1	0	1	0.00	0.00	0.00	0.00	0.00	251.00
NFKB1	1	0	1	0.00	0.00	0.00	0.00	0.00	251.00
NFKB2	1	0	1	0.00	0.00	0.00	0.00	0.00	251.00
NOS1	1	0	1	0.00	0.00	0.00	0.00	0.00	251.00
ORM1	1	0	1	0.00	0.00	0.00	0.00	0.00	116.00
PAWR	1	0	1	0.00	0.00	0.00	0.00	0.00	251.00
PFN1	1	0	1	0.00	0.00	0.00	0.00	0.00	251.00
PHB1	1	0	1	0.00	0.00	0.00	0.00	0.00	116.00
Pi3	1	0	1	0.00	0.00	0.00	0.00	0.00	3.00
PLA2G2A	1	0	1	0.00	0.00	0.00	0.00	0.00	251.00
PLAU	1	0	1	0.00	0.00	0.00	0.00	0.00	251.00
PPPR15A	1	0	1	0.00	0.00	0.00	0.00	0.00	251.00
PRKCI	1	0	1	0.00	0.00	0.00	0.00	0.00	251.00
PRKCZ	1	0	1	0.00	0.00	0.00	0.00	0.00	251.00
PRKD1	1	0	1	0.00	0.00	0.00	0.00	0.00	116.00
Proteasome	1	0	1	0.00	0.00	0.00	0.00	0.00	251.00
PSMB9	1	0	1	0.00	0.00	0.00	0.00	0.00	251.00
PSME1	1	0	1	0.00	0.00	0.00	0.00	0.00	251.00
PTGES	1	0	1	0.00	0.00	0.00	0.00	0.00	251.00
PTHlh	1	0	1	0.00	0.00	0.00	0.00	0.00	251.00
PTX3	1	0	1	0.00	0.00	0.00	0.00	0.00	251.00
RELA	1	0	1	0.00	0.00	0.00	0.00	0.00	251.00
RIPK1	1	0	1	0.00	0.00	0.00	0.00	0.00	251.00
RIPK3	1	0	1	0.00	0.00	0.00	0.00	0.00	251.00
SELE	1	0	1	0.00	0.00	0.00	0.00	0.00	251.00
SERPINE1	1	0	1	0.00	0.00	0.00	0.00	0.00	251.00
SERPING1	1	0	1	0.00	0.00	0.00	0.00	0.00	251.00
SERPINH1	1	0	1	0.00	0.00	0.00	0.00	0.00	251.00
SLC6A4	1	0	1	0.00	0.00	0.00	0.00	0.00	251.00
SLC6A6	1	0	1	0.00	0.00	0.00	0.00	0.00	251.00
SMPD1	1	0	1	0.00	0.00	0.00	0.00	0.00	251.00
SOCS1	1	0	1	0.00	0.00	0.00	0.00	0.00	38.00
SP1	1	0	1	0.00	0.00	0.00	0.00	0.00	251.00
SPP1	1	0	1	0.00	0.00	0.00	0.00	0.00	251.00
ST3GAL6	1	0	1	0.00	0.00	0.00	0.00	0.00	251.00
BMX	0	1	1	0.00	0.31	0.00	5.00	3.26	38.00
ETS1	0	1	1	0.00	0.31	0.00	5.00	3.26	38.00
FGFR1	0	1	1	0.00	0.31	0.00	5.00	3.26	38.00
FGFR3	0	1	1	0.00	0.31	0.00	5.00	3.26	38.00
HDAC	0	1	1	0.00	0.31	0.00	5.00	3.26	38.00
HDAC1	0	1	1	0.00	0.31	0.00	5.00	3.26	38.00
HDAC2	0	1	1	0.00	0.31	0.00	5.00	3.26	38.00
HDAC3	0	1	1	0.00	0.31	0.00	5.00	3.26	38.00
IFNGR1	0	1	1	0.00	0.31	0.00	5.00	3.26	38.00
IFNL1	0	1	1	0.00	0.31	0.00	5.00	3.26	38.00
IFNL2	0	1	1	0.00	0.31	0.00	5.00	3.26	38.00
JAK2	0	1	1	0.00	0.31	0.00	5.00	3.26	38.00
LPL	0	1	1	0.00	0.31	0.00	5.00	3.26	38.00
PDGFRB	0	1	1	0.00	0.31	0.00	5.00	3.26	38.00
PRKCD	0	1	1	0.00	0.31	0.00	5.00	3.26	38.00
PRKCE	0	1	1	0.00	0.31	0.00	5.00	3.26	38.00
PRMT1	0	1	1	0.00	0.31	0.00	5.00	3.26	38.00
RET	0	1	1	0.00	0.31	0.00	5.00	3.26	38.00
TYK2	0	1	1	0.00	0.31	0.00	5.00	3.26	38.00
STAT2	1	0	1	0.00	0.00	0.00	0.00	0.00	116.00
TAP1	1	0	1	0.00	0.00	0.00	0.00	0.00	251.00
TAP2	1	0	1	0.00	0.00	0.00	0.00	0.00	251.00
THBS1	1	0	1	0.00	0.00	0.00	0.00	0.00	251.00
TIMP1	1	0	1	0.00	0.00	0.00	0.00	0.00	251.00
ADAM17	0	1	1	0.00	0.39	0.00	4.00	2.54	251.00
AGTR1	0	1	1	0.00	0.39	0.00	4.00	2.54	251.00
AKR1B1	0	1	1	0.00	0.39	0.00	4.00	2.54	251.00
ALOX5	0	1	1	0.00	0.39	0.00	4.00	2.54	251.00
Caspase	0	1	1	0.00	0.39	0.00	4.00	2.54	251.00
CENPJ	0	1	1	0.00	0.39	0.00	4.00	2.54	251.00
DCN	0	1	1	0.00	0.39	0.00	4.00	2.54	251.00

DCTN1	0	1	1	0.00	0.39	0.00	4.00	2.54	251.00
DHX9	0	1	1	0.00	0.39	0.00	4.00	2.54	251.00
EGR4	0	1	1	0.00	0.39	0.00	4.00	2.54	251.00
HMGGB1	0	1	1	0.00	0.39	0.00	4.00	2.54	251.00
HNRNPU	0	1	1	0.00	0.39	0.00	4.00	2.54	251.00
HSPA4	0	1	1	0.00	0.39	0.00	4.00	2.54	251.00
HSPB1	0	1	1	0.00	0.39	0.00	4.00	2.54	251.00
ICMT	0	1	1	0.00	0.39	0.00	4.00	2.54	251.00
IRF9	0	1	1	0.00	0.39	0.00	4.00	2.54	251.00
MAP3K7	0	1	1	0.00	0.39	0.00	4.00	2.54	251.00
MMP12	0	1	1	0.00	0.39	0.00	4.00	2.54	251.00
NAMPT	0	1	1	0.00	0.39	0.00	4.00	2.54	251.00
NFAT	0	1	1	0.00	0.39	0.00	4.00	2.54	251.00
NOX4	0	1	1	0.00	0.39	0.00	4.00	2.54	251.00
NRAS	0	1	1	0.00	0.39	0.00	4.00	2.54	251.00
OLR1	0	1	1	0.00	0.39	0.00	4.00	2.54	251.00
PDE3B	0	1	1	0.00	0.39	0.00	4.00	2.54	251.00
PLA2G4A	0	1	1	0.00	0.39	0.00	4.00	2.54	251.00
RALBP1	0	1	1	0.00	0.39	0.00	4.00	2.54	251.00
TARDBP	0	1	1	0.00	0.39	0.00	4.00	2.54	251.00
TONSL	0	1	1	0.00	0.39	0.00	4.00	2.54	251.00
TP53	1	0	1	0.00	0.00	0.00	0.00	0.00	251.00
TRAF1	1	0	1	0.00	0.00	0.00	0.00	0.00	251.00
TRAF3	1	0	1	0.00	0.00	0.00	0.00	0.00	251.00
TRAF6	1	0	1	0.00	0.00	0.00	0.00	0.00	16.00
TRPV1	1	0	1	0.00	0.00	0.00	0.00	0.00	3.00
TYMP	1	0	1	0.00	0.00	0.00	0.00	0.00	251.00
VIM	1	0	1	0.00	0.00	0.00	0.00	0.00	251.00
ABCc2	1	0	1	0.00	0.00	0.00	0.00	0.00	251.00
AHSG	1	0	1	0.00	0.00	0.00	0.00	0.00	116.00
ALB	1	0	1	0.00	0.00	0.00	0.00	0.00	116.00
APOE	1	0	1	0.00	0.00	0.00	0.00	0.00	116.00
C3AR1	1	0	1	0.00	0.00	0.00	0.00	0.00	251.00
CASP9	1	0	1	0.00	0.00	0.00	0.00	0.00	116.00
CCND1	1	0	1	0.00	0.00	0.00	0.00	0.00	7.00
ZNF175	0	1	1	0.00	0.30	0.00	5.00	3.29	10.00
CD33	1	0	1	0.00	0.00	0.00	0.00	0.00	116.00
CP	1	0	1	0.00	0.00	0.00	0.00	0.00	251.00
CST3	1	0	1	0.00	0.00	0.00	0.00	0.00	251.00
CTTNB1	1	0	1	0.00	0.00	0.00	0.00	0.00	251.00
ERG	1	0	1	0.00	0.00	0.00	0.00	0.00	251.00
F12	1	0	1	0.00	0.00	0.00	0.00	0.00	116.00
FOXO1	1	0	1	0.00	0.00	0.00	0.00	0.00	116.00
FSCN1	1	0	1	0.00	0.00	0.00	0.00	0.00	251.00
GADD45A	1	0	1	0.00	0.00	0.00	0.00	0.00	116.00
GLI3	1	0	1	0.00	0.00	0.00	0.00	0.00	5.00
IGFBP3	1	0	1	0.00	0.00	0.00	0.00	0.00	251.00
BMP6	0	1	1	0.00	0.28	0.00	6.00	3.52	116.00
GH1	0	1	1	0.00	0.28	0.00	6.00	3.52	116.00
MEOX2	0	1	1	0.00	0.28	0.00	6.00	3.52	116.00
PPARG	0	1	1	0.00	0.28	0.00	6.00	3.52	116.00
SOD1	0	1	1	0.00	0.28	0.00	6.00	3.52	116.00
INSR	1	0	1	0.00	0.00	0.00	0.00	0.00	251.00
JUP	1	0	1	0.00	0.00	0.00	0.00	0.00	251.00
NCOA1	1	0	1	0.00	0.00	0.00	0.00	0.00	116.00
NFKBIB	1	0	1	0.00	0.00	0.00	0.00	0.00	251.00
NOS2	1	0	1	0.00	0.00	0.00	0.00	0.00	251.00
OCLN	1	0	1	0.00	0.00	0.00	0.00	0.00	251.00
PDE4	1	0	1	0.00	0.00	0.00	0.00	0.00	5.00
PPM1B	1	0	1	0.00	0.00	0.00	0.00	0.00	251.00
PROCR	1	0	1	0.00	0.00	0.00	0.00	0.00	251.00
PROS1	1	0	1	0.00	0.00	0.00	0.00	0.00	116.00
RB1	1	0	1	0.00	0.00	0.00	0.00	0.00	251.00
RETN	1	0	1	0.00	0.00	0.00	0.00	0.00	251.00
SCARB1	1	0	1	0.00	0.00	0.00	0.00	0.00	251.00
SCD	1	0	1	0.00	0.00	0.00	0.00	0.00	251.00
SLC10A1	1	0	1	0.00	0.00	0.00	0.00	0.00	251.00
SLC2A4	1	0	1	0.00	0.00	0.00	0.00	0.00	251.00
SLC01A2	1	0	1	0.00	0.00	0.00	0.00	0.00	251.00
PIAS1	0	1	1	0.00	0.31	0.00	5.00	3.26	38.00
TERT	1	0	1	0.00	0.00	0.00	0.00	0.00	19.00
TFAP2C	1	0	1	0.00	0.00	0.00	0.00	0.00	251.00
THBD	1	0	1	0.00	0.00	0.00	0.00	0.00	251.00
AMPK	0	1	1	0.00	0.39	0.00	4.00	2.54	251.00
EGF	0	1	1	0.00	0.39	0.00	4.00	2.54	251.00
IL10RA	0	1	1	0.00	0.39	0.00	4.00	2.54	251.00
P2RY6	0	1	1	0.00	0.39	0.00	4.00	2.54	251.00
PEBP1	0	1	1	0.00	0.39	0.00	4.00	2.54	251.00
PIAS3	0	1	1	0.00	0.39	0.00	4.00	2.54	251.00
PNPLA3	0	1	1	0.00	0.39	0.00	4.00	2.54	251.00
PRKCH	0	1	1	0.00	0.39	0.00	4.00	2.54	251.00
RHOB	0	1	1	0.00	0.39	0.00	4.00	2.54	251.00
RNF216	0	1	1	0.00	0.39	0.00	4.00	2.54	251.00
SALL4	0	1	1	0.00	0.39	0.00	4.00	2.54	251.00
SERPINA1	0	1	1	0.00	0.39	0.00	4.00	2.54	251.00
SFTP1A	0	1	1	0.00	0.39	0.00	4.00	2.54	251.00
SH3BGRL3	0	1	1	0.00	0.39	0.00	4.00	2.54	251.00
SOD2	0	1	1	0.00	0.39	0.00	4.00	2.54	251.00
TNFAIP3	0	1	1	0.00	0.39	0.00	4.00	2.54	251.00
TXN	0	1	1	0.00	0.39	0.00	4.00	2.54	251.00
USP31	0	1	1	0.00	0.39	0.00	4.00	2.54	251.00
VIPR2	0	1	1	0.00	0.39	0.00	4.00	2.54	251.00
XIAP	0	1	1	0.00	0.39	0.00	4.00	2.54	251.00
ZFAND5	0	1	1	0.00	0.39	0.00	4.00	2.54	251.00
ZFP36	0	1	1	0.00	0.39	0.00	4.00	2.54	251.00

**Table S3.** Replicate fine-tuning results for BERT, Llama 1B and Llama 3B parameter LLM

BERT Model replicate trials							Llama 3.2 1B Model replicate trials									
	Trial #1	Trial #2	Trial #3	Trial #4	Trial #5	Average	Std Error		Trial #1	Trial #2	Trial #3	Trial #4	Trial #5	Average	Std Error	p value wrt BERT
Total Positive Questions	23	23	23	23	23	23.00	0.00		23	23	23	23	23	23.00	0.00	
Total Negative Questions	23	23	23	23	23	23.00	0.00		0	23	13	23	0	11.80	5.15	
Total Correct Positive	15	15	21	0	5	11.20	3.80		23	0	11	0	23	11.40	5.14	
Total Correct Negative	14	10	6	23	16	13.80	2.87									
Overall Accuracy Positive (%)	65.22	65.22	91.30	0.00	21.74	48.70	16.52		0.00	100.00	56.52	100.00	0.00	51.30	22.40	0.928
Overall Accuracy Negative (%)	60.87	43.48	26.09	100.00	69.57	60.00	12.48		100.00	0.00	47.83	0.00	100.00	49.57	22.36	0.697
Overall Accuracy (%)	63.04	54.35	58.70	50.00	45.65	54.35	3.07		50.00	50.00	52.17	50.00	50.00	50.43	0.43	0.274
Average Entropy Positive	0.91	0.87	1.00	1.00	0.96	0.95	0.02		0.96	0.32	0.02	0.26	0.58	0.43	0.16	0.031
Average Entropy Negative	0.89	0.85	1.00	1.00	0.83	0.91	0.04		0.96	0.32	0.02	0.26	0.61	0.43	0.16	0.040

**Table S4.** Active learning recruitment of new examples

Name	Indegree	Outdegree	EdgeCount	Trial #1 Correct High E + incorrect low E			Trial #2 Correct High E + incorrect low E			Trial #3 Correct High E + incorrect low E			Trial #4 Increased low E only			Trial #5 Increased low E only			Trial #6 Increased low entropy			Trial #7 Increased low entropy		
				Frequency vs Source	Frequency vs Target	Frequency vs tail	Frequency vs Source	Frequency vs Target	Frequency vs tail	Frequency vs Source	Frequency vs Target	Frequency vs tail	Frequency vs Source	Frequency vs Target	Frequency vs tail	Frequency vs Source	Frequency vs Target	Frequency vs tail	Frequency vs Source	Frequency vs Target	Frequency vs tail	Frequency vs Source	Frequency vs Target	Frequency vs tail
TNF	59	67	126	21	8	13	12	15	12	33	16	10	11	12	7	34	7	11	12	11	1	4	1	
IL6	55	72	20	5	2	5	1	3	1	3	5	7	2	5	2	1	3	2	1	1	1	0	0	
CRP	13	7	20	2	1	2	1	0	0	1	4	0	0	1	0	1	1	0	1	1	0	0	0	
MYD88	10	7	17	0	0	0	0	0	0	4	0	0	0	0	0	0	0	0	0	0	0	0	0	
CDA14	3	11	0	0	0	0	0	0	0	4	0	0	0	0	0	0	0	0	0	0	0	0	0	
NFkappaB	6	4	10	0	0	0	0	0	0	0	0	0	0	0	0	0	0	0	0	0	0	0	0	
IRF3	7	3	10	1	0	1	1	0	0	0	1	1	0	0	0	1	1	1	1	1	1	0	0	
IRF5	2	5	7	1	0	1	0	1	1	0	1	1	1	1	1	1	1	1	1	1	1	1	1	
IFNG	4	2	6	1	0	1	0	0	0	0	1	0	0	0	0	1	0	0	0	0	0	0	0	
TLR9	1	4	5	0	0	0	0	0	0	0	1	0	0	0	0	0	0	0	0	0	0	0	0	
PRPF8	1	5	5	0	0	0	0	0	0	0	1	0	0	0	0	0	0	0	0	0	0	0	0	
AGT	1	3	4	0	0	0	0	0	0	1	1	0	0	0	0	0	0	0	0	0	0	0	0	
IFNA1	2	2	4	1	1	1	1	0	1	0	1	1	1	1	1	1	1	1	1	1	1	0	0	
IL1B	3	4	1	0	0	0	0	0	0	1	1	1	1	1	1	1	1	1	1	1	1	0	0	
EGFR	2	2	4	0	0	0	0	0	0	1	1	1	1	1	1	1	1	1	1	1	1	0	0	
STAT3	2	2	4	0	0	0	0	0	0	1	0	0	0	0	0	0	0	0	0	0	0	0	0	
MAPK3	2	2	4	0	0	0	0	0	0	1	0	0	0	0	0	0	0	0	0	0	0	0	0	
MAPK3	2	2	4	0	0	0	0	0	0	1	0	0	0	0	0	0	0	0	0	0	0	0	0	
TLR2	2	2	4	0	0	0	0	0	0	1	0	0	0	0	0	0	0	0	0	0	0	0	0	
API	3	3	5	0	0	0	0	0	0	0	0	0	0	0	0	0	0	0	0	0	0	0	0	
CA2	3	0	3	0	0	0	0	0	0	0	0	0	0	0	0	0	0	0	0	0	0	0	0	
CCDC102G	2	1	5	0	0	0	0	0	0	1	0	0	0	0	0	0	0	0	0	0	0	0	0	
ERK	1	2	3	0	0	0	0	0	0	1	0	0	0	0	0	0	0	0	0	0	0	0	0	
p38	0	3	3	0	0	0	0	0	0	1	0	0	0	0	0	0	0	0	0	0	0	0	0	
PFD32	1	2	3	0	0	0	0	0	0	1	0	0	0	0	0	0	0	0	0	0	0	0	0	
CXCL12	1	2	3	0	0	0	0	0	0	1	0	0	0	0	0	0	0	0	0	0	0	0	0	
ESR1	3	0	3	0	0	0	0	0	0	1	0	0	0	0	0	0	0	0	0	0	0	0	0	
ULTA	1	2	3	1	0	0	0	0	0	1	0	0	0	0	0	0	0	0	0	0	0	0	0	
IL18	1	2	3	0	0	0	0	0	0	1	0	0	0	0	0	0	0	0	0	0	0	0	0	
NEST	1	2	3	0	0	0	0	0	0	1	0	0	0	0	0	0	0	0	0	0	0	0	0	
INS	0	3	3	0	0	0	0	0	0	1	0	0	0	0	0	0	0	0	0	0	0	0	0	
NGF	0	3	3	0	0	0	0	0	0	1	0	0	0	0	0	0	0	0	0	0	0	0	0	
TRAF3	1	2	3	0	0	0	0	0	0	1	0	0	0	0	0	0	0	0	0	0	0	0	0	
IRF3	1	2	3	0	0	0	0	0	0	1	0	0	0	0	0	0	0	0	0	0	0	0	0	
TRAF1	1	2	3	0	0	0	0	0	0	1	0	0	0	0	0	0	0	0	0	0	0	0	0	
P02P2	2	1	3	1	0	0	0	0	0	2	0	1	0	0	0	0	0	0	0	0	0	0	0	
ADPOQ	1	1	3	0	0	0	0	0	0	1	0	0	0	0	0	0	0	0	0	0	0	0	0	
ABCB1	2	0	2	0	0	0	0	0	0	1	0	0	0	0	0	0	0	0	0	0	0	0	0	
PKE	0	2	2	0	0	0	0	0	0	0	1	0	0	0	0	0	0	0	0	0	0	0	0	
CASPB	2	0	2	0	0	0	0	0	0	1	0	0	0	0	0	0	0	0	0	0	0	0	0	
PRAK	1	1	2	0	0	0	0	0	0	1	0	0	0	0	0	0	0	0	0	0	0	0	0	
HCK	1	1	2	0	0	0	0	0	0	1	0	0	0	0	0	0	0	0	0	0	0	0	0	
HGT1	2	0	2	0	0	0	0	0	0	1	0	0	0	0	0	0	0	0	0	0	0	0	0	
IRFB1	1	1	2	1	0	0	0	0	0	1	1	0	0	0	0	0	0	0	0	0	0	0	0	
IRKB1	1	1	2	1	0	0	0	0	0	1	1	0	0	0	0	0	0	0	0	0	0	0	0	
IRKB2	1	1	2	1	0	0	0	0	0	1	1	0	0	0	0	0	0	0	0	0	0	0	0	
TNFRSF1A	1	1	2	0	0	0	0	0	0	1	0	0	0	0	0	0	0	0	0	0	0	0	0	
VIF	0	2	2	0	0	0	0	0	0	1	0	0	0	0	0	0	0	0	0	0	0	0	0	
XDE	1	1	2	0	0	0	0	0	0	1	0	0	0	0	0	0	0	0	0	0	0	0	0	
IRAK2	1	1	2	0	0	0	0	0	0	1	0	0	0	0	0	0	0	0	0	0	0	0	0	
MAP2K3	1	1	2	0	0	0	0	0	0	1	0	0	0	0	0	0	0	0	0	0	0	0	0	
MAP2K3	1	1	2	0	0	0	0	0	0	1	0	0	0	0	0	0	0	0	0	0	0	0	0	
TUFA1	0	2	2	0	0	0	0	0	0	1	0	0	0	0	0	0	0	0	0	0	0	0	0	
PDMC	1	1	2	1	0	0	0	0	0	1	0	0	0	0	0	0	0	0	0	0	0	0	0	
PDR	1	1	2	0	0	0	0	0	0	1	0	0	0	0	0	0	0	0	0	0	0	0	0	
PRKA	2	0	2	2	0	0	0	0	0	1	0	0	0	0	0	0	0	0	0	0	0	0	0	
RORA	1	1	2	0	0	0	0	0	0	1	0	0	0	0	0	0	0	0	0	0	0	0	0	
SOC33	0	2	2	0	0	0	0	0	0	1	0	0	0	0	0	0	0	0	0	0	0	0	0	
ADRB2	0	2	2	0	0	0	0	0	0	1	0	0	0	0	0	0	0	0	0	0	0	0	0	
ABC11	1	0	1	0	0	0	0	0	0	1	0	0	0	0	0	0	0	0	0	0	0	0	0	
ABC12	1	0	1	0	0	0	0	0	0	1	0	0	0	0	0	0	0	0	0	0	0	0	0	
ADAMTS5	1	0	1	0	0	0	0	0	0	1	0	0	0	0	0	0	0	0	0	0	0	0	0	
AKT1	1	0	1	0	0	0	0	0	0	1	0	0	0	0	0	0	0	0	0	0	0	0	0	
AKT2	1	0	1	0	0	0	0	0	0	1	0	0	0	0	0	0	0	0	0	0	0	0	0	
AKL	1	0	1	0	0	0	0	0	0	1	0	0	0	0	0	0	0	0	0	0	0	0	0	
ANXA1	1	0	1	0	0	0	0	0	0	1	0	0	0	0	0	0	0	0	0	0	0	0	0	
AREG	1	0	1	0	0	0	0	0	0	1	0	0	0	0	0	0	0	0	0	0	0	0	0	
ATF2	1	0	1	0	0	0	0	0	0	1	0	0	0	0	0	0	0	0	0	0	0	0	0	
ATF3	1	0	1	0	0	0	0	0	0	1	0	0	0	0	0	0	0	0	0	0	0	0	0	
BAP2	1	0	1	0	0	0	0	0	0	1	0	0	0	0	0	0	0	0	0	0	0	0	0	
CBP	1	0	1	0	0	0	0	0	0	1	0	0	0	0	0	0	0	0	0	0	0	0	0	
KT10	0	1	1	0	0	0	0	0	0	1	0	0	0	0	0	0	0	0	0	0	0	0	0	
CD163	1	0	1	0	0	0	0	0	0	1	0	0	0	0	0	0	0	0	0	0	0	0	0	
CD56	1	0	1	0	0	0	0	0	0	1	0	0	0	0	0	0	0	0	0	0	0	0	0	
CD59	1	0	1	0	0	0	0	0	0	1	0	0	0	0	0	0	0	0	0	0	0	0	0	
CD86	1	0	1</td																					



ZFAND5	0	1	1	0	0	0	0	0
ZFP38	0	0	0	0	0	0	0	0
<hr/>								
Unique Sources	30	26	21	26	28	25	20	20
Unique Targets	44	41	40	40	47	37	38	38
Total Unique	43	74	66	66	75	57	58	58

0	0	1	0	0	0	0	0	0
0	0	0	0	0	0	0	0	0
<hr/>								
Unique Sources	26	28	25	25	29	29	20	20
Unique Targets	19	19	37	37	15	38	38	38
Total Unique	49	75	51	57	44	58	0.81	0.63

p-values

Unique Sources	Unique Targets	
Edge Count > 1	0.81	0.77
Edge Count = 1	0.62	0.66
Total Unique	0.81	0.63

**Table S5.** Sources and targets with high and low edge count recruited uniquely by each policy

Name	EdgeCount	Sources unique to High/ Low Entropy	Targets unique to High/ Low Entropy	Sources unique to Low Entropy	Targets unique to Low Entropy
TNF	273	0	0	0	0
IL6	126	0	0	0	0
STAT1	42	0	0	0	0
CRP	20	0	0	0	0
MYD88	17	0	0	1	0
CD14	11	0	0	0	0
NFKappaB	10	0	0	0	0
IRF3	10	0	0	0	0
IFI16	7	0	0	0	0
IFNG	6	0	0	0	1
TLR9	5	1	0	0	0
PTPA	5	0	0	0	0
AGT	4	1	0	0	1
IFNA1	4	0	0	0	0
IL1B	4	0	0	0	0
EGFR	4	0	0	1	0
STAT3	4	0	1	0	0
MAPK1	4	0	0	1	0
MAPK3	4	0	0	0	0
TLR2	4	1	0	0	0
AP1	3	1	0	0	0
CA2	3	0	1	0	0
CCL2	3	0	0	0	1
CD40LG	3	0	0	0	0
ERK	3	0	0	0	0
p38	3	0	0	0	0
PTGS2	3	0	0	0	1
CXCL12	3	1	0	0	0
ESR1	3	0	0	0	0
IL17A	3	0	0	0	0
IL18	3	0	0	0	0
IL6ST	3	1	0	0	0
INS	3	0	0	0	0
NGF	3	0	0	0	0
TLR4	3	0	0	0	0
TLR3	3	0	0	0	0
IRF5	3	0	0	1	0
TBK1	3	0	0	0	0
POU2F1	3	0	0	0	0
ADIPQ	3	0	0	1	0
ABCB1	2	0	0	0	0
PKC	2	1	0	0	0
CASP8	2	0	0	0	0
P13K	2	0	0	0	0
PRAKAC	2	1	0	0	0
CD1A	2	0	1	0	0
CD40	2	0	0	0	0
CDKN1A	2	0	0	0	0
CEBPB	2	0	0	0	1
CHUK	2	1	0	0	1
CXCL8	2	0	0	0	0
EP300	2	0	0	0	1
CAMP	2	0	0	0	0
GSK3B	2	0	0	0	0
HCK	2	0	0	0	0
HSF1	2	0	1	0	0
IFNB1	2	0	0	0	0
IKBKB	2	0	0	0	0
IKBKG	2	0	0	0	0
ADRB2	2	0	0	1	0
BSG	2	0	0	0	0
ERBB2	2	0	0	0	0
IL13	2	0	0	0	0
IL4	2	0	0	0	0
OSM	2	1	0	0	0
PARP1	2	1	0	0	0
PTK2	2	0	0	0	0
PTPN11	2	0	0	0	0
TGFBI	2	0	0	0	0
TNFRSF1A	2	0	0	1	0
VEGF	2	1	0	0	0
XDH	2	0	0	0	0
IRAK1	2	0	0	0	1
IRF7	2	0	0	0	0
MAP3K1	2	0	0	0	0
MAPK14	2	0	0	0	0
TLR1	2	0	0	1	0
POMC	2	0	0	0	0
PTEN	2	0	0	0	0
RIPK2	2	1	1	0	0
RORA	2	0	0	0	0
SERPINA3	2	0	0	0	0
IL10	2	0	0	0	0
TGFA	2	0	0	0	0
TIMP3	2	0	1	0	0
NFKBIA	2	1	0	0	0
NOS3	2	0	0	0	0
TRAF2	2	0	0	0	0
TNFRSF1B	2	0	0	0	0
VCAM1	2	0	0	0	0
VEGFA	2	0	1	0	0
AKT	2	0	0	0	0
PPARA	2	0	0	1	0
SCOS3	2	0	0	0	0
ADRB	2	0	0	1	0
A2M	1	0	0	0	0
ABCC1	1	0	0	0	0
ABCg2	1	0	0	0	1
ADAMTS5	1	0	0	0	1
AIM2	1	0	1	0	0
AKT1	1	0	0	0	0
AKT2	1	0	0	0	0
ALPL	1	0	0	0	1
ANXA1	1	0	0	0	0
AREG	1	0	0	0	0

Edge Count >1

ATF2	1	0	0	0	0	0
ATF3	1	0	0	0	0	0
BMP2	1	0	0	0	0	0
C1R	1	0	0	0	0	1
C3	1	0	0	0	0	0
C5AR1	1	0	0	0	0	0
C8A	1	0	0	0	0	0
C8G	1	0	1	0	0	0
NKX2-1	1	0	0	0	0	0
CASP1	1	0	0	0	0	0
CASP2	1	0	0	0	0	0
CASP6	1	0	1	0	0	0
CASP7	1	0	0	0	0	0
CBL	1	0	0	0	0	1
CCL11	1	0	1	0	0	0
CCL3	1	0	0	0	0	0
CCR2	1	0	0	0	0	0
CEBP	1	1	0	0	0	0
KITLG	1	0	0	0	0	0
CD163	1	0	0	0	0	1
CD38	1	0	0	0	0	1
CD55	1	0	0	0	0	1
CD59	1	0	0	0	0	0
CD80	1	0	0	0	0	0
CD86	1	0	0	0	0	0
CDKN1B	1	0	0	0	0	0
CFB	1	0	0	0	0	0
CFL2	1	0	0	0	0	1
CK2	1	0	0	0	0	1
CLEC3B	1	0	0	0	0	0
CLIC4	1	0	0	0	0	0
CMA1	1	0	0	0	0	0
CD32	1	0	0	0	0	0
HNF1A	1	0	0	0	0	0
LEP	1	0	0	0	0	0
CSF1	1	0	0	0	0	0
CSF2	1	0	0	0	0	0
CSF3	1	0	0	0	0	1
CTSB	1	0	0	0	0	0
CTSL	1	0	0	0	0	0
CTSS	1	0	0	0	0	0
CX3CL1	1	0	0	0	0	0
CXCL10	1	0	0	0	0	1
CXCL5	1	0	0	0	0	1
CXCL9	1	0	0	0	0	0
CXCR3	1	0	1	0	0	0
DAPK1	1	0	0	0	0	0
EHF	1	0	0	0	0	0
F2RL1	1	0	0	0	0	0
F2RL3	1	0	0	0	0	0
FAS	1	0	0	0	0	0
FCER2	1	0	0	0	0	0
FCGR1A	1	0	0	0	0	0
FCGR3B	1	0	0	0	0	0
FN1	1	0	0	0	0	0
FOXO4	1	0	0	0	0	1
FUT4	1	0	0	0	0	0
FYN	1	0	0	0	0	1
GBF1	1	0	0	0	0	0
HBEGF	1	0	0	0	0	0
HIF1A	1	0	0	0	0	0
HLA-A	1	0	1	0	0	0
HLA-B	1	0	0	0	0	0
HLA-C	1	0	0	0	0	0
HLA-F	1	0	1	0	0	0
HP	1	0	1	0	0	0
HSD11B1	1	0	0	0	0	1
HSP90B1	1	0	0	0	0	0
HOXD3	1	0	0	0	0	0
LIF	1	1	0	0	0	0
RAF1	1	0	0	1	0	0
IKK_family	1	0	0	0	0	0
IL11	1	0	1	0	0	0
IL12A	1	0	0	0	0	0
IL12B	1	0	0	0	0	1
IL4R	1	0	0	0	0	0
AHR	1	0	0	0	0	0
AR	1	0	0	0	0	0
F10	1	0	0	0	0	0
F2	1	0	0	0	0	0
GAB1	1	0	0	0	0	0
IL17F	1	1	0	0	0	0
IL1R1	1	0	0	1	0	0
IL6R	1	0	0	0	0	0
ITGA5	1	0	0	0	0	0
KLF7	1	0	0	0	0	0
LEPR	1	0	0	0	0	0
LMX1B	1	0	0	0	0	0
PIK3C3	1	0	0	0	0	0
PNPT1	1	0	0	0	0	0
PTGER4	1	0	0	0	0	0
TIRAP	1	0	0	0	0	0
IRAK4	1	0	0	0	0	1
BEGAIN	1	0	0	1	0	0
IKBKE	1	0	0	0	0	0
MAVS	1	0	0	0	0	0
TICAM1	1	0	0	0	0	0
ITGA6	1	0	0	0	0	0
ITGAV	1	0	0	0	0	0
JAK	1	0	0	0	0	0
JUN	1	0	0	0	0	1
KRAS	1	0	0	0	0	0
LYN	1	0	1	0	0	0
LYZ	1	0	0	0	0	0
MAP2K1	1	0	0	0	0	1
MAP2K2	1	0	0	0	0	0
MAP2K6	1	0	0	0	0	0
MAP3K14	1	0	0	0	0	0

MAP3K5	1	0	0	0	0	0
MAP4K3	1	0	1	0	0	0
MAP4K4	1	0	0	0	0	0
MAPK7	1	0	0	0	0	0
MAPK9	1	0	0	0	0	1
MAP3K14	1	0	0	0	0	0
MAZ	1	0	0	0	0	0
MEF2	1	0	1	0	0	0
MGAT4B	1	0	1	0	0	0
MGAT5	1	0	0	0	0	1
MIF	1	0	0	0	0	0
MMP1	1	0	0	0	0	0
MMP14	1	0	0	0	0	0
MMP3	1	0	0	0	0	0
MMP9	1	0	0	0	0	0
MUC5AC	1	0	0	0	0	0
TLR5	1	0	0	0	0	0
TLR6	1	0	0	0	0	0
TLR7	1	0	0	1	0	0
TLR8	1	0	0	0	0	0
MYLK	1	0	0	0	0	0
NCAM1	1	0	0	0	0	0
NFKB1	1	0	0	0	0	0
NFKB2	1	0	0	0	0	0
NOS1	1	0	0	0	0	0
ORM1	1	0	1	0	0	0
PAWR	1	0	0	0	0	0
PFN1	1	0	1	0	0	0
PHB1	1	0	1	0	0	0
P13	1	0	0	0	0	0
PLA2G2A	1	0	0	0	0	1
PLAU	1	0	0	0	0	0
PPP1R15A	1	0	0	0	0	0
PRKCI	1	0	0	0	0	0
PRKCZ	1	0	0	0	0	0
PRKD1	1	0	0	0	0	0
Proteasome	1	0	0	0	0	0
PSMB9	1	0	0	0	0	0
PSME1	1	0	0	0	0	0
PTGES	1	0	0	0	0	0
PTHlh	1	0	0	0	0	0
PTX3	1	0	0	0	0	0
RELA	1	0	0	0	0	1
RIPK1	1	0	0	0	0	0
RIPK3	1	0	0	0	0	0
SELE	1	0	0	0	0	0
SERpine1	1	0	0	0	0	0
SERPING1	1	0	0	0	0	0
SERPINH1	1	0	0	0	0	1
SLC6A4	1	0	0	0	0	0
SLC6A6	1	0	0	0	0	0
SMPD1	1	0	0	0	0	0
SOCs1	1	0	0	0	0	0
SP1	1	0	1	0	0	0
SP1P1	1	0	0	0	0	0
ST3GAL6	1	0	0	0	0	0
BMX	1	0	0	0	0	0
ETS1	1	0	0	0	0	0
FGFR1	1	0	0	1	0	0
FGFR3	1	1	0	0	0	0
HDAC	1	0	0	0	0	0
HDAC1	1	0	0	0	0	0
HDAC2	1	0	0	0	0	0
HDAC3	1	0	0	0	0	0
IFNGR1	1	0	0	0	0	0
IFNL1	1	1	0	0	0	0
IFNL2	1	1	0	0	0	0
JAK2	1	0	0	1	0	0
LPL	1	0	0	0	0	0
PDGFRB	1	0	0	0	0	0
PRKCD	1	0	0	0	0	0
PRKCE	1	0	0	0	0	0
PRMT1	1	0	0	1	0	0
RET	1	0	0	1	0	0
TYK2	1	0	0	0	0	0
STAT2	1	0	0	0	0	0
TAP1	1	0	0	0	0	0
TAP2	1	0	0	0	0	0
THBS1	1	0	0	0	0	0
TIMP1	1	0	0	0	0	1
ADAM17	1	0	0	0	0	0
AGTR1	1	0	0	0	0	0
AKR1B1	1	0	0	1	0	0
ALOX5	1	0	0	0	0	0
Caspase	1	0	0	0	0	0
CENPJ	1	0	0	0	0	0
DCN	1	0	0	0	0	0
DCTN1	1	0	0	0	0	0
DHX9	1	0	0	0	0	0
EGR4	1	0	0	0	0	0
HMGBl	1	0	0	1	0	0
HNRNPU	1	0	0	0	0	0
HSPA4	1	1	0	0	0	0
HSPB1	1	0	0	1	0	0
ICMT	1	0	0	1	0	0
IRF9	1	1	0	0	0	0
MAP3K7	1	0	0	0	0	0
MMP12	1	0	0	0	0	0
NAMPT	1	0	0	0	0	0
NFAT	1	1	0	0	0	0
NOX4	1	0	0	1	0	0
NRAS	1	0	0	1	0	0
OLR1	1	0	0	0	0	0
PDE3B	1	1	0	0	0	0
PLA2G4A	1	1	0	0	0	0
RALBP1	1	0	0	0	1	0
TARDBP	1	0	0	0	0	0
TONSL	1	0	0	0	0	0

	1	0	1	0	0
TP53	1	0	0	0	0
TRAF1	1	0	0	0	0
TRAF3	1	0	0	0	1
TRAF6	1	0	0	0	0
TRPV1	1	0	0	0	0
TYMP	1	0	0	0	1
VIM	1	0	1	0	0
ABCC2	1	0	0	0	0
AHSG	1	0	0	0	0
ALB	1	0	1	0	0
APOE	1	0	0	0	0
C3AR1	1	0	0	0	0
CASP9	1	0	0	0	0
CCND1	1	0	0	0	0
ZNF175	1	0	0	0	0
CD33	1	0	0	0	0
CP	1	0	0	0	0
CST3	1	0	0	0	0
CTNNB1	1	0	0	0	0
ERG	1	0	0	0	1
F12	1	0	0	0	0
FOXO1	1	0	0	0	0
FSCN1	1	0	0	0	0
GADD45A	1	0	0	0	0
GL3	1	0	0	0	0
ICFBP3	1	0	0	0	0
BMP6	1	0	0	0	0
GH1	1	0	0	0	0
MEOX2	1	1	0	0	0
PPARG	1	0	0	0	0
SOD1	1	0	0	0	0
INSR	1	0	0	0	0
JUP	1	0	0	0	0
NCOA1	1	0	0	0	0
NFKB1B	1	0	1	0	0
NOS2	1	0	0	0	1
OCLN	1	0	0	0	0
PDE4	1	0	1	0	0
PPM1B	1	0	0	0	0
PROCR	1	0	0	0	0
PROS1	1	0	0	0	0
RB1	1	0	0	0	0
RETN	1	0	1	0	0
SCARB1	1	0	0	0	0
SCD	1	0	0	0	0
SLC10A1	1	0	0	0	0
SLC2A4	1	0	0	0	0
SLCO1A2	1	0	0	0	0
PIAS1	1	0	0	0	0
TERT	1	0	0	0	0
TFAP2C	1	0	0	0	0
THBD	1	0	1	0	0
AMPK	1	0	0	0	0
EGF	1	0	0	0	0
IL10RA	1	1	0	0	0
P2RY6	1	1	0	0	0
PEBP1	1	0	0	0	0
PIAS3	1	0	0	0	0
PNPLA3	1	1	0	0	0
PRKCH	1	0	0	0	0
RHOB	1	0	0	1	0
RNF216	1	0	0	0	0
SALL4	1	0	0	0	0
SERPINA1	1	0	0	0	0
SFTPA1	1	0	0	0	0
SH3BGR13	1	0	0	0	0
SOD2	1	0	0	0	0
TNFAIP3	1	0	0	1	0
TXN	1	0	0	0	0
USP31	1	0	0	0	0
VIPR2	1	0	0	1	0
XIAP	1	1	0	0	0
ZFAND5	1	0	0	1	0
ZFP36	1	0	0	0	0
	Sources Unique to High/Low Entropy		Targets Unique to High/Low Entropy		
	14		7		
	Sources Unique to Low Entropy		Targets Unique to Low Entropy		
	10		8		Edge Count > 1
	16		24		
	19		30		Edge Count = 1

**Table S6.** Sources and targets with high and low neighborhood connectivity recruited uniquely by each policy

Name	EdgeCount	Neighborhood Connectivity	Sources unique to High/ Low Entropy	Targets unique to High/ Low Entropy	Sources unique to Low Entropy	Targets unique to Low Entropy
CHUK	2	251.00	1	0	0	1
IKBKB	2	251.00	0	0	0	0
IKBKG	2	251.00	0	0	0	0
MAP3K1	2	251.00	0	0	0	0
PTEN	2	251.00	0	0	0	0
RIPK2	2	251.00	1	1	0	0
TIMP3	2	251.00	0	0	0	0
NOS3	2	251.00	0	0	0	0
TRAF2	2	251.00	0	0	0	0
TNFRSF1B	2	251.00	0	0	0	0
AKT2	1	251.00	0	0	0	0
APL	1	251.00	0	0	0	1
AREG	1	251.00	0	0	0	0
ATF1	1	251.00	0	0	0	0
ATF3	1	251.00	0	0	0	0
BMP2	1	251.00	0	0	0	0
C1R	1	251.00	0	0	0	1
C3	1	251.00	0	0	0	0
CSAR1	1	251.00	0	0	0	0
CASP1	1	251.00	0	0	0	0
CASP2	1	251.00	0	0	0	0
CASP6	1	251.00	0	1	0	0
CASP7	1	251.00	0	0	0	0
CCL11	1	251.00	0	1	0	0
CCL3	1	251.00	0	0	0	0
CD38	1	251.00	0	0	0	1
CD55	1	251.00	0	0	0	1
CD59	1	251.00	0	0	0	0
CD80	1	251.00	0	0	0	0
CD86	1	251.00	0	0	0	0
CFB	1	251.00	0	0	0	0
CFL2	1	251.00	0	0	0	1
CK2	1	251.00	0	0	0	1
CLEC3B	1	251.00	0	0	0	0
CLIC4	1	251.00	0	0	0	0
CSF1	1	251.00	0	0	0	0
CSF2	1	251.00	0	0	0	0
CSF3	1	251.00	0	0	0	1
CTSB	1	251.00	0	0	0	0
CX3CL1	1	251.00	0	0	0	0
CXC110	1	251.00	0	0	0	1
CXCL5	1	251.00	0	0	0	1
CXCL9	1	251.00	0	0	0	0
CXR2	1	251.00	0	1	0	0
DAPR	1	251.00	0	0	0	0
EHF	1	251.00	0	0	0	0
F2RL1	1	251.00	0	0	0	0
F2RL3	1	251.00	0	0	0	0
FAS	1	251.00	0	0	0	0
FCER2	1	251.00	0	0	0	0
FCGR3B	1	251.00	0	0	0	0
FOXO4	1	251.00	0	0	0	1
FUT4	1	251.00	0	0	0	0
HIF1A	1	251.00	0	0	0	0
HLA-A	1	251.00	0	1	0	0
HLA-B	1	251.00	0	0	0	0
HLA-C	1	251.00	0	0	0	0
HLA-F	1	251.00	0	0	0	0
HSD11B1	1	251.00	0	0	0	1
IL11	1	251.00	0	1	0	0
IL12A	1	251.00	0	0	0	0
IL12B	1	251.00	0	0	0	1
IL4R	1	251.00	0	0	0	0
ITGA6	1	251.00	0	0	0	0
ITGAV	1	251.00	0	0	0	0
JAK	1	251.00	0	0	0	0
JUN	1	251.00	0	0	0	1
LYZ	1	251.00	0	0	0	0
MAP2K1	1	251.00	0	0	0	1
MAP2K2	1	251.00	0	0	0	0
MAP2K6	1	251.00	0	0	0	0
MAP3K14	1	251.00	0	0	0	0
MAP3K5	1	251.00	0	0	0	0
MAP4K3	1	251.00	0	1	0	0
MAP4K4	1	251.00	0	0	0	0
MAPK9	1	251.00	0	0	0	1
MAPKAPK3	1	251.00	0	0	0	0
MIF	1	251.00	0	0	0	0
MMP1	1	251.00	0	0	0	0
MMP14	1	251.00	0	0	0	0
MUC5AC	1	251.00	0	0	0	0
MYLK	1	251.00	0	0	0	0
NCAM1	1	251.00	0	0	0	0
NFKB1	1	251.00	0	0	0	0
NFKB2	1	251.00	0	0	0	0
NOS1	1	251.00	0	0	0	0
PAWR	1	251.00	0	0	0	0
PFN1	1	251.00	0	1	0	0
PLA2G2A	1	251.00	0	0	0	1
PLAU	1	251.00	0	0	0	0
PPP1R15A	1	251.00	0	0	0	0
PRKC1	1	251.00	0	0	0	0
PRKC2	1	251.00	0	0	0	0
Proteasome	1	251.00	0	0	0	0
PSMB9	1	251.00	0	0	0	0
PSME1	1	251.00	0	0	0	0
PTGES	1	251.00	0	0	0	0
PTH1H	1	251.00	0	0	0	0
PTX3	1	251.00	0	0	0	0
RELA	1	251.00	0	0	0	1
RIPK1	1	251.00	0	0	0	0
RIPK2	1	251.00	0	0	0	0
SELE	1	251.00	0	0	0	0
SERPINE1	1	251.00	0	0	0	0
SERPING1	1	251.00	0	0	0	0
SERPINH1	1	251.00	0	0	0	1
SLC6A4	1	251.00	0	0	0	0
SLC6A6	1	251.00	0	0	0	0
SMPD7	1	251.00	0	0	0	0
SP1	1	251.00	0	1	0	0
SPP1	1	251.00	0	0	0	0
ST3GAL6	1	251.00	0	0	0	0
TAP1	1	251.00	0	0	0	0
TAP2	1	251.00	0	0	0	0
THBS1	1	251.00	0	0	0	0
TIMP1	1	251.00	0	0	0	1
ADAM17	1	251.00	0	0	0	0
AGR1	1	251.00	0	0	0	0
AKR1B1	1	251.00	0	0	1	0
ALOX5	1	251.00	0	0	0	0
Caspase	1	251.00	0	0	0	0
CENP1	1	251.00	0	0	0	0
DCN	1	251.00	0	0	0	0
DCTN1	1	251.00	0	0	0	0
DHX9	1	251.00	0	0	0	0
EGR4	1	251.00	0	0	0	0
HMG61	1	251.00	0	0	1	0
HNRNPU	1	251.00	0	0	0	0
HSPA4	1	251.00	1	0	0	0
HSPB1	1	251.00	0	0	1	0

Neighborhood Connectivity = max or 251

ICMT	1	251.00	0	0	1	0
IRF9	1	251.00	1	0	0	0
MAP3K7	1	251.00	0	0	0	0
MMP12	1	251.00	0	0	0	0
NAMPT	1	251.00	0	0	0	0
NFAT	1	251.00	1	0	0	0
NOX4	1	251.00	0	0	1	0
NRAS	1	251.00	0	0	1	0
OLR1	1	251.00	0	0	0	0
PDE3B	1	251.00	1	0	0	0
PLA2G4A	1	251.00	1	0	0	0
RALBP1	1	251.00	0	0	0	0
TARDBP	1	251.00	0	0	1	0
TONSL	1	251.00	0	0	0	0
TP53	1	251.00	0	1	0	0
TRAFA1	1	251.00	0	0	0	0
TRAF3	1	251.00	0	0	0	1
TYMP	1	251.00	0	0	0	1
VIM	1	251.00	0	1	0	0
ABC2C2	1	251.00	0	0	0	0
C3AR1	1	251.00	0	0	0	0
CP	1	251.00	0	0	0	0
CST3	1	251.00	0	0	0	0
CTNNB1	1	251.00	0	0	0	0
ERG	1	251.00	0	0	0	1
FSCN1	1	251.00	0	0	0	0
IGFBP3	1	251.00	0	0	0	0
INSR	1	251.00	0	0	0	0
JUP	1	251.00	0	0	0	0
NFKBIB	1	251.00	0	1	0	0
NOS2	1	251.00	0	0	0	1
OCLN	1	251.00	0	0	0	0
PPM1B	1	251.00	0	0	0	0
PROCR	1	251.00	0	0	0	0
RB1	1	251.00	0	0	0	0
RETN	1	251.00	0	1	0	0
SCARB1	1	251.00	0	0	0	0
SCD	1	251.00	0	0	0	0
SLC10A1	1	251.00	0	0	0	0
SLC2A4	1	251.00	0	0	0	0
SLC01A2	1	251.00	0	0	0	0
TFAP2C	1	251.00	0	0	0	0
THBD	1	251.00	0	1	0	0
AMPK	1	251.00	0	0	0	0
EGF	1	251.00	0	0	0	0
IL10RA	1	251.00	1	0	0	0
P2RY6	1	251.00	1	0	0	0
P2RP1	1	251.00	0	0	0	0
PIAS3	1	251.00	0	0	0	0
PNP1A3	1	251.00	1	0	0	0
PRKCH	1	251.00	0	0	0	0
RHOB	1	251.00	0	0	1	0
RNF216	1	251.00	0	0	0	0
SALL4	1	251.00	0	0	0	0
SERPINA1	1	251.00	0	0	0	0
SETPA1	1	251.00	0	0	0	0
SH3BGLL3	1	251.00	0	0	0	0
SOD2	1	251.00	0	0	0	0
TNFAIP3	1	251.00	0	0	1	0
TXN	1	251.00	0	0	0	0
USP31	1	251.00	0	0	0	0
VIPR2	1	251.00	0	0	1	0
XIAP	1	251.00	1	0	0	0
ZFAND5	1	251.00	0	0	1	0
ZFP36	1	251.00	0	0	0	0
CD40LG	3	183.50	0	0	0	0
IL17A	3	183.50	0	0	0	0
IL18	3	183.50	0	0	0	0
INS	3	183.50	0	0	0	0
POU2F1	3	183.50	0	0	0	0
ADIPQ	3	183.50	0	0	1	0
ABC1	2	183.50	0	0	0	0
CD1A	2	183.50	0	1	0	0
CD40	2	183.50	0	0	0	0
CEBPB	2	183.50	0	0	0	1
HSP1	2	183.50	0	1	0	0
ADRB	2	183.50	0	0	1	0
BSC	2	183.50	0	0	0	0
ERRB2	2	183.50	0	0	0	0
IL13	2	183.50	0	0	0	0
PARP1	2	183.50	1	0	0	0
PTK2	2	183.50	0	0	0	0
TNFRSF1A	2	183.50	0	0	1	0
VEGF	2	183.50	1	0	0	0
XDH	2	183.50	0	0	0	0
MAPK14	2	183.50	0	0	0	0
RORA	2	183.50	0	0	0	0
SERPINA3	2	183.50	0	0	0	0
VEGFA	2	183.50	0	1	0	0
CDKN1A	2	144.50	0	0	0	0
IL10	2	144.50	0	0	0	0
ADRB	2	144.50	0	0	1	0
EGFR	4	135.00	0	0	1	0
MAPK3	4	135.00	0	0	0	0
PTGS2	3	135.00	0	0	0	1
ESR1	3	135.00	0	0	0	0
NFKBIA	2	135.00	1	0	0	0
VCAM1	2	135.00	0	0	0	0
CASP8	2	133.50	0	0	0	0
TLR1	2	133.50	0	0	1	0
EP300	2	130.50	0	0	0	1
IFNB1	2	130.50	0	0	0	0
IL1B	4	128.67	0	0	0	0
CCL2	3	128.67	0	0	0	1
TGF&	2	128.00	0	0	0	0
G93B	2	126.50	0	0	0	0
CXCL12	3	125.67	1	0	0	0
TLR4	3	125.67	0	0	0	0
STAT3	4	124.67	0	1	0	0
API	3	123.33	1	0	0	0
AGT	4	122.67	1	0	0	1
NGF	3	122.67	0	0	0	0
HCK	2	116.00	0	0	0	0
POMC	2	116.00	0	0	0	0
A2M	1	116.00	0	0	0	0
ABCC1	1	116.00	0	0	0	0
ABCG2	1	116.00	0	0	0	1
ADAMTS5	1	116.00	0	0	0	1
AKT1	1	116.00	0	0	0	0
ANXA1	1	116.00	0	0	0	0
C8A	1	116.00	0	0	0	0
C8G	1	116.00	0	1	0	0
CBL	1	116.00	0	0	0	1
CD163	1	116.00	0	0	0	1
CDKN1B	1	116.00	0	0	0	0
CMA1	1	116.00	0	0	0	0
CTSL	1	116.00	0	0	0	0
CTSS	1	116.00	0	0	0	0
FN1	1	116.00	0	0	0	0
FYN	1	116.00	0	0	0	1
GBF1	1	116.00	0	0	0	0
HBEGF	1	116.00	0	0	0	0
HP	1	116.00	0	1	0	0
HSP90B1	1	116.00	0	0	0	0

AHR	1	116.00	0	0	0	0
AR	1	116.00	0	0	0	0
F10	1	116.00	0	0	0	0
F2	1	116.00	0	0	0	0
GAB1	1	116.00	0	0	0	0
IL17F	1	116.00	1	0	0	0
IL1R1	1	116.00	0	0	1	0
IL6R	1	116.00	0	0	0	0
ITGA5	1	116.00	0	0	0	0
KLF7	1	116.00	0	0	0	0
LEPR	1	116.00	0	0	0	0
LMX1B	1	116.00	0	0	0	0
PIK3C3	1	116.00	0	0	0	0
PNP1	1	116.00	0	0	0	0
PTGER4	1	116.00	0	0	0	0
IRAP	1	116.00	0	0	0	0
RSAS	1	116.00	0	0	0	0
LIN	1	116.00	0	1	0	0
MAPK7	1	116.00	0	0	0	0
MAZ	1	116.00	0	0	1	0
MEF2	1	116.00	0	1	0	0
MGAT4B	1	116.00	0	1	0	0
MGAT5	1	116.00	0	0	0	1
MMP9	1	116.00	0	0	0	0
ORM1	1	116.00	0	1	0	0
PHB1	1	116.00	0	1	0	0
PRKD1	1	116.00	0	0	0	0
STAT2	1	116.00	0	0	0	0
AHSG	1	116.00	0	0	0	0
ALB	1	116.00	0	1	0	0
APOE	1	116.00	0	0	0	0
CASP9	1	116.00	0	0	0	0
CD33	1	116.00	0	0	0	0
F12	1	116.00	0	0	0	0
FOXO1	1	116.00	0	0	0	0
GADD45A	1	116.00	0	0	0	0
BMP6	1	116.00	0	0	0	0
GH1	1	116.00	0	0	0	0
MEOX2	1	116.00	1	0	0	0
PPARG	1	116.00	0	0	0	0
SOD1	1	116.00	0	0	0	0
NCOA1	1	116.00	0	0	0	0
PROS1	1	116.00	0	0	0	0
MAPK1	4	102.50	0	0	1	0
TLR2	4	92.33	1	0	0	0
IFNL4	6	85.60	0	0	0	1
IL6ST	3	77.00	1	0	0	0
CSM1	2	77.00	1	0	0	0
PTPN11	2	77.00	0	0	0	0
SOC3S	2	77.00	0	0	0	0
IL4	2	67.50	0	0	0	0
PPARA	2	67.50	0	0	1	0
PI3K	2	63.00	0	0	0	0
TGFBI	2	63.00	0	0	0	0
AKT	2	60.50	0	0	0	0
PKC	2	59.50	1	0	0	0
NFKappaB	10	57.13	0	0	0	0
ERK	3	46.67	0	0	0	0
p38	3	45.33	0	0	0	0
SOC31	1	38.00	0	0	0	0
BMX	1	38.00	0	0	0	0
ETS1	1	38.00	0	0	0	0
FGR1	1	38.00	0	0	1	0
FGR3	1	38.00	1	0	0	0
HDAC	1	38.00	0	0	0	0
HDAC1	1	38.00	0	0	0	0
HDAC2	1	38.00	0	0	0	0
HDAC3	1	38.00	0	0	0	0
IFNGR1	1	38.00	0	0	0	0
IFNL1	1	38.00	1	0	0	0
IFNL2	1	38.00	1	0	0	0
JAK2	1	38.00	0	0	1	0
LPL	1	38.00	0	0	0	0
PDGFRB	1	38.00	0	0	0	0
PRKCD	1	38.00	0	0	0	0
PRKCE	1	38.00	0	0	0	0
PRMT1	1	38.00	0	0	1	0
RET	1	38.00	0	0	1	0
TYK2	1	38.00	0	0	0	0
PIAS1	1	38.00	0	0	0	0
IF16	7	27.57	0	0	0	0
CD14	11	27.40	0	0	0	0
IRF5	3	27.00	0	0	1	0
IRAK1	2	27.00	0	0	0	1
CRP	20	21.32	0	0	0	0
IFNA1	4	19.33	0	0	0	0
CCR2	1	19.00	0	0	0	0
CD32	1	19.00	0	0	0	0
HNF1A	1	19.00	0	0	0	0
LEP	1	19.00	0	0	0	0
FCGR1A	1	19.00	0	0	0	0
TERT	1	19.00	0	0	0	0
IKK_family	1	16.00	0	0	0	0
IRAK4	1	16.00	0	0	0	1
TLR5	1	16.00	0	0	0	0
TLR6	1	16.00	0	0	0	0
TLR7	1	16.00	0	0	1	0
TLR8	1	16.00	0	0	0	0
TRAF6	1	16.00	0	0	0	0
CXCL8	2	12.00	0	0	0	0
IRF7	2	10.50	0	0	0	0
CEBP	1	10.00	1	0	0	0
KTIG	1	10.00	0	0	0	0
BEGAIN	1	10.00	0	0	1	0
IEK1	1	10.00	0	0	0	0
MAN1	1	10.00	0	0	0	0
TICAM1	1	10.00	0	0	0	0
ZNF175	1	10.00	0	0	0	0
STAT1	42	8.39	0	0	0	0
HDXD3	1	7.00	0	0	0	0
U1F	1	7.00	1	0	0	0
RAF1	1	7.00	0	0	1	0
CCND1	1	7.00	0	0	0	0
TLR9	5	6.00	1	0	0	0
TLR3	3	6.00	0	0	0	0
PRKAC	2	6.00	1	0	0	0
TBK1	3	5.00	0	0	0	0
GLI3	1	5.00	0	0	0	0
PDE4	1	5.00	0	1	0	0
AIM2	1	3.00	0	1	0	0
NKX2-1	1	3.00	0	0	0	0
P13	1	3.00	0	0	0	0
TRPV1	1	3.00	0	0	0	0
MYD88	17	2.38	0	0	1	0
PTPA	5	2.20	0	0	0	0
CA2	3	2.00	0	1	0	0
CAMP	2	2.00	0	0	0	0
IRF3	10	1.90	0	0	0	0
IL6	126	1.79	0	0	0	0
TNF	273	1.57	0	0	0	0

Sources Unique to High/Low Entropy Targets Unique to High/Low Entropy

11 16

Sources Unique to Low Entropy Targets Unique to Low Entropy

11 24 Neighborhood Connectivity = max

19 35

18 14 Neighborhood Connectivity < max